

LLMTrack: Semantic Multi-Object Tracking with Multi-modal Large Language Model

Pan Liao, Feng Yang, Di Wu, Jinwen Yu, Yuhua Zhu, Wenhui Zhao, and Dingwen Zhang

Northwestern Polytechnical University, Xi'an, China

Abstract. Multi-Object Tracking (MOT) is evolving from geometric localization to Semantic MOT (SMOT) to answer complex relational queries, yet progress is hindered by semantic data scarcity and a structural disconnect between tracking architectures and Multi-modal Large Language Models (MLLMs). To address this, we introduce Grand-SMOT, a large-scale, open-world benchmark providing high-density, dual-stream narratives that comprehensively decouple individual behaviors from environmental contexts. Furthermore, we propose LLMTrack, the first framework to seamlessly integrate MLLMs into the SMOT task. LLMTrack establishes a Macro-Understanding-First paradigm, utilizing a novel Spatio-Temporal Fusion Module to align discrete geometric trajectories with continuous semantic features, effectively suppressing temporal hallucinations during online processing. Extensive experiments demonstrate that LLMTrack achieves state-of-the-art geometric tracking performance while delivering a qualitative leap in dynamic semantic reasoning. Notably, our analysis reveals that high-quality semantic narratives empower the language model to deduce complex social interactions naturally, demonstrating that direct cognitive reasoning is more effective than cumbersome explicit visual modeling. Ultimately, our contributions bridge the gap between perceptual tracking and cognitive reasoning, establishing a robust new foundation for comprehensive video understanding and intelligent narrative generation.

Keywords: Semantic Multi-Object Tracking · Multi-modal Large Language Model

1 Introduction

Multi-Object Tracking (MOT) traditionally focuses on spatial localization answering "*where objects are*" [12, 23, 32, 39, 63, 65]. However, as AI advances toward Generalization, mere coordinates cannot satisfy the profound demands of intelligent video analytics [49, 60, 61]. This necessitates a paradigm shift from Geometric Perception to Semantic Reasoning. While recent pioneering efforts have explored dynamic prompt modeling [66] and MLLM-driven motion alignment for Referring MOT [30], we posit the need for a more holistic Semantic Multi-Object Tracking (SMOT) [22] system. Such a system must track targets while concurrently answering "*what they are doing*," "*how appearances evolve*,"

and "what happens contextually." Although Multi-modal Large Language Models (MLLMs) [1, 17, 46, 50, 59] excel in static image understanding, adapting them to the dynamic SMOT task presents a dual challenge: severe data scarcity and a fundamental architectural disconnect.

The efficacy of large models is inherently data-driven [11, 16]; yet, the current SMOT landscape suffers from a structural deficiency in high-quality instruction-tuning data. Existing datasets fail to meet the scale required for training billion-parameter models and, more critically, suffer from Semantic Scarcity. They often settle for brief category tags or shallow, single-sentence descriptions, neglecting the deep characterization of video-level atmosphere and instance-level dynamics, which has been shown to severely limit [6]. Furthermore, we identify a philosophical limitation in prior work [22], which treat *Interaction* as a predefined recognition task. Attempting to teach models relationships through explicit supervision is, we argue, semantically redundant. From a first-principles perspective, interaction is not independent metadata but a natural logical deduction arising from the collision between individual behaviors and environmental context [51]. When a model can exhaustively parse "what the individual is doing" and "what is occurring in the environment," the so-called interaction should be deconstructed as an emergent capability [54, 64], rather than relying on rigid label injection.

Guided by this insight, we introduce Grand-SMOT, a new large-scale benchmark designed to balance the depth of interaction with the breadth of an open world. Rather than building from scratch, we strategically integrated and reshaped two mainstream data sources. First, we performed a deep semantic expansion on BenSMOT [22], upgrading its mechanical interaction tags into rich, context-aware narratives. Second, addressing the data-hungry nature of foundation models, we incorporated the TAO dataset [7]. Our selection of TAO extends far beyond its sheer volume; it serves as a critical anchor for realism. Unlike traditional MOT datasets confined to specific, controlled scenarios (*e.g.*, pedestrians or traffic), TAO captures the raw, unscripted complexity of the real world. This choice aligns Grand-SMOT with the evolving demands of the mainstream community, positioning the SMOT task not merely as an extension of traditional tracking, but as a pivotal bridge to Open World MOT a modern-

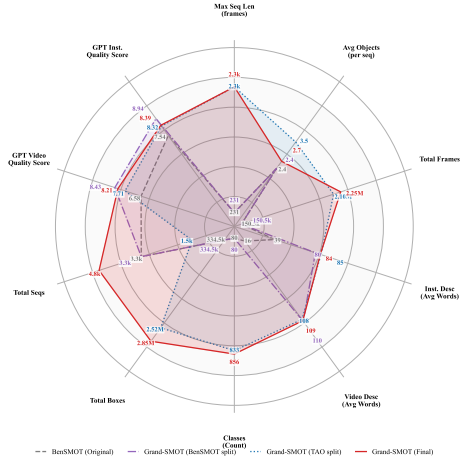


Fig. 1: Statistical Comparison. We visualize the data distribution of our Grand-SMOT against BenSMOT [22]. Grand-SMOT achieves a superior balance in sequence length, instance density, and semantic richness.

ized paradigm essential for generalized tracking in unconstrained environments. Regarding the annotation strategy, drawing inspiration from recent advanced data engines [5, 6], we abandoned traditional interaction classification in favor of a dense re-annotation strategy. We established a supervision paradigm centered on dual-stream dense descriptions (decoupling Individual Behavior from Environmental Context). Through a unified hierarchical generation pipeline, we homogenized these heterogeneous data sources into high-density semantic assets containing environmental atmosphere, fine-grained dynamics, and causal logic. This strategy not only breaks existing scale bottlenecks but also ensures dual coverage of complex interactions and atypical open-world objects, laying a solid foundation for training cognitive trackers with strong generalization capabilities.

However, high-quality data alone is insufficient. Existing MLLMs [1, 17, 59] are predominantly trained on static images and lack an inherent perception of temporal logic. To bridge this gap, we propose LLMTrack. Addressing the open-world nature of Grand-SMOT, we employ Grounding DINO [27] as the frontend visual anchor to ensure alignment between low-level object detection and the high-level open semantic space. On this basis, LLMTrack establishes a "*Macro-Understanding-First, Micro-Tracking-Follows*" cognitive paradigm. Far from a simple stacking of modules, it leverages LLaVA-OneVision [17] and LLaVA-OneVision-1.5 [1] to first parse the Global Context of the video, using it as a prior to guide specific instance association. To facilitate this, we designed a Spatio-Temporal Fusion Module, which utilizes an adaptive attention mechanism to map discrete geometric trajectories into continuous features readable by the large model. This effectively suppresses temporal hallucinations and empowers the model to engage in robust long-term reasoning.

In summary, the core contributions of this paper are as follows:

1. We propose **LLMTrack**, the first tracking framework to integrate MLLMs into the SMOT task. It establishes a **Macro-Understanding-First** cognitive paradigm and incorporates a **Spatio-Temporal Fusion Module** to effectively align geometric trajectories with semantic reasoning, suppressing temporal hallucinations.
2. We introduce **Grand-SMOT**, a large-scale benchmark constructed by homogenizing the TAO and BenSMOT datasets. It resolves the semantic scarcity issue by offering high-density, open-world semantic assets that encompass both environmental atmosphere and fine-grained dynamics.

2 Related Work

2.1 From Geometric Association to Semantic Reasoning

Traditional MOT has predominantly focused on the geometric consistency of trajectories. Early approaches relied on Kalman filtering and strictly spatial heuristics for association [3, 57], while recent advances have shifted toward purely learned association metrics [36, 65] and end-to-end Transformer architectures [12, 33, 63]. Despite their success in maintaining identity across frames, these

methods fundamentally treat objects as bounding boxes without semantic comprehension, limiting their utility in high-level tasks such as Embodied AI. To bridge this gap, recent works explore tracking-by-language paradigms [32, 49], such as aligning dynamic motion modalities via MLLMs for Referring MOT [30] or leveraging explicit and implicit prompt modeling for state adaptation [66]. Notably, Li et al. [22] formalized the SMOT task to output both trajectories and dense captions. However, their discriminative BERT-based [9] method treats interaction recognition as a closed-set classification problem. This lacks the generative reasoning and open-world generalization inherent in modern LLMs, restricting the depth of semantic interpretation in complex environments.

2.2 Large Multi-modal Models in Dynamic Video Understanding

Although Large Multi-modal Models (LMMs) [1, 46] excel in static image understanding [6, 26], extending frame-level detection architectures like LLMDet [10] to continuous videos inevitably induces temporal hallucinations and identity fragmentation. Conversely, video-specific LMMs [19, 64] manage computational costs via aggressive token compression, sacrificing the fine-grained motion details critical for tracking. Compounding this architectural challenge is a data bottleneck: existing datasets [7, 14] offer sparse labels rather than the dense causal narratives needed to train cognitive trackers. We address these dual limitations by leveraging LLaVA-OneVision [1, 17] to preserve high-fidelity visual cues, coupled with our novel dense-captioned benchmark to unlock MLLMs’ temporal reasoning capabilities.

3 The Grand-SMOT Dataset

Constructing a cognitive tracking benchmark requires transcending the geometric constraints of traditional datasets. We introduce **Grand-SMOT**, a large-scale semantic tracking benchmark designed to address the semantic scarcity in current MOT research. As summarized in Table 1, Grand-SMOT distinguishes itself by providing high-density spatio-temporal narratives that support the proposed *Macro-Understanding-First* paradigm, significantly outperforming existing benchmarks in both semantic granularity and scale.

3.1 Data Formulation and Philosophy

Departing from prior methodologies that reduce interaction to rigid classification labels, we reframe interaction as a logical deduction emerging from the interplay between an agent and its environment (detailed interaction modeling is provided in the Appendix). Formally, each training sample is defined as a triplet $\mathcal{S} = (V, \mathcal{T}_{env}, \mathcal{T}_{ins})$. Here, V denotes the video sequence, while \mathcal{T}_{env} represents the **Video-Level Caption**, capturing the global atmosphere, weather conditions, and scene context. We explicitly decouple this from $\mathcal{T}_{ins} = \{(b_i, d_i)\}_{i=1}^K$, the **Instance-Level Caption**, where d_i chronicles the i -th target’s appearance

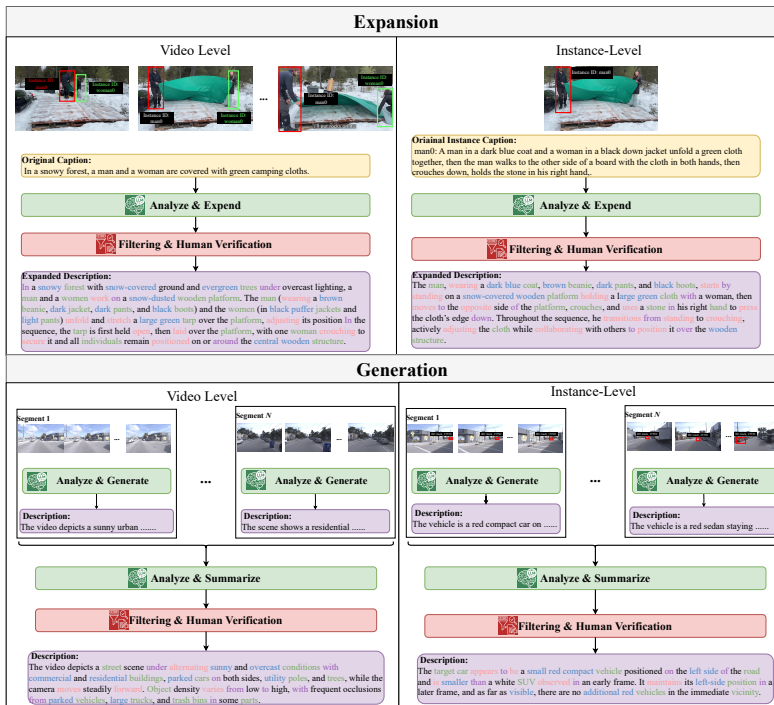


Fig. 2: Our pipeline uses **Expansion** (top) to upgrade sparse labels to rich descriptions, and **Generation** (bottom) to synthesize video and instance dynamics via a segment-to-global approach.

evolution and fine-grained micro-actions. This dual-stream structure compels the tracker to implicitly reason about relations, rather than merely memorizing biased label co-occurrences.

3.2 Unified Generation Pipeline

Creating such dense annotations from scratch is prohibitively expensive. Therefore, we designed a unified pipeline (Figure 2) that adapts to the distinct characteristics of two mainstream datasets: BenSMOT [22] and TAO [7]. We utilize Qwen3-VL-32B [59], currently one of the leading open-source MLLMs, as our core semantic engine to ensure high-quality text generation (comprehensive ablation studies comparing different MLLMs are provided in the Appendix).

(1) Semantic Expansion: We formulate the expansion of BenSMOT as a conditional generative mapping $\Phi : (s, v) \rightarrow \mathcal{N}_{dense}$, where a sparse interaction tag s serves as a semantic anchor rooted in the visual context v . This mapping function Φ executes a **Semantic Densification** process: it conditions the narrative generation on extracted environmental priors \mathcal{E} (e.g., atmospheric conditions, scene layout) and fine-grained visual attributes. By embedding the rigid interaction label into this continuous, high-dimensional context, Φ transforms isolated tags into cohesive, visually grounded narratives that vividly encapsulate the target’s presence within the scene.

Table 1: Comparison with representative MOT and tracking benchmarks. **Sem.:** Semantic annotation level. **Inst.:** Instance-level descriptions. **Env.:** Video-level environmental context. **Grand-SMOT (Ours)** is the only benchmark offering dual-stream dense narratives with open-world coverage.

Dataset	Classes	Scale			Semantic Granularity	
		Videos	Tracks	Frames	Inst. Desc.	Env. Context
MOT17 [34]	1	14	1.3K	11K	×	×
MOT20 [8]	1	8	3.8K	13K	×	×
DanceTrack [43]	1	100	990	106K	×	×
GroOT [35]	8	1.5k	13.3K	2.2M	Brief Sent.	×
TAO [7]	833	1.5K	17.3K	2.1M	Class Name	×
BenSMOT [22]	80	3.3K	7.8K	151K	Interaction Tag	Brief Sent.
Grand-SMOT (Ours)	854[†]	4.8K*	25K*	2.3M*	Dense Narrative	Dense Narrative

[†]: The number of non-overlapping classes in the merged TAO and BenSMOT taxonomy. * : Approximate sum of integrated sources (TAO + BenSMOT).

(2) Hierarchical Generation: For TAO dataset, we propose a bottom-up paradigm to resolve long-sequence forgetting. We discretize the video stream into non-overlapping segments $\mathbf{S} = \{S_k\}_{k=1}^N$. To rigorously prevent label leakage from TAO’s noisy taxonomy (*e.g.*, generic "baby" labels), we define a visual-only generation function $d_k = \mathcal{G}(I(S_k, b) \mid \emptyset_{text})$, which explicitly conditions strictly on the visual region $I(\cdot)$ while enforcing an empty textual prior \emptyset_{text} . Subsequently, a global fusion operator $\mathcal{T}_{global} = \mathcal{F}(\{d_k\}_{k=1}^N)$ aggregates these fragmented local descriptions, synthesizing a coherent narrative that preserves instance identity and temporal continuity across the entire sequence.

3.3 Quality Assurance

Cognizant of the hallucination risks inherent in MLLMs and the prohibitive costs of full manual verification, we enforce a strict, cost-effective quality assurance protocol. To effectively mitigate self-evaluation bias, we decouple generation from verification by employing an independent Vision-Language Critic (*e.g.*, MiniCPM-V 4.0 [47]). The Critic computes a fine-grained cross-modal alignment score (on a 1 to 10 scale) to directly evaluate the semantic fidelity, temporal coherence, and physical correctness between the raw video sequence and the generated narrative. Sequences scoring below an empirically established threshold ($\tau = 7.0$) are automatically flagged as “hard cases” and routed for manual refinement. Quantitatively, this automated filtering flagged approximately 5% of the dataset (255 videos), successfully capturing over 90% of severe temporal hallucinations. To resolve these boundary cases, expert annotators spent 20 hours manually inspecting and rectifying specific error types, such as identity switches and phantom actions. This Human-in-the-Loop verification achieved a high inter-annotator agreement (Cohen’s $\kappa = 0.85$), with an ultimate human acceptance and refinement rate of **94%**. Consequently, this targeted hybrid strategy strictly confines manual intervention to complex scenarios, ensuring human-level physical correctness while drastically optimizing annotation costs. Post-verification,

the final benchmark retains exactly **4,770** verified sequences (exact counts are detailed in Table 1). Concrete examples of human corrections, sequence length and category distributions, and comprehensive protocol formulations are deferred to the **Appendix**.

4 LLMtrack

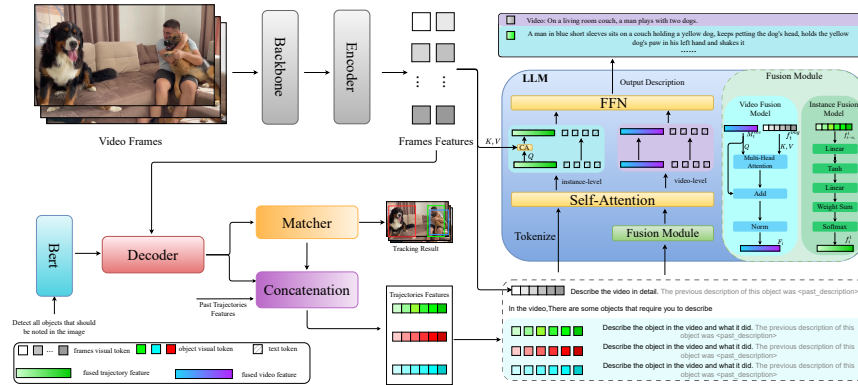


Fig. 3: LLMTrack architecture. Online processing uses backbone visual features and tracker instance features in a Fusion Module (Video Fusion for long-term context, Instance Fusion for short-term dynamics). Fused tokens + previous-frame description enable LLM to generate current-frame narratives via Cross-Attention (CA), which integrates features during single-object captioning.

4.1 Overview

We formulate SMOT as a dual-branch online process involving continuous geometric association and semantic reasoning. Let $\mathcal{V} = \{I_1, I_2, \dots, I_T\}$ denote a streaming video sequence. At each time step t , the system performs two concurrent tasks: (1) **Geometric Tracking**, yielding the spatial coordinates $B_t = \{b_t^i\}_{i=1}^{N_t}$ and identities for all active targets; and (2) **Semantic Interpretation**, generating a comprehensive state description \mathcal{S}_t .

To achieve efficient online tracking, we adopt the Joint Detection and Embedding (JDE) [53] paradigm for our visual frontend. As illustrated in Figure 3, **LLMTrack** consists of this visual frontend, a Spatio-Temporal Fusion Module, and an LMM backend. To establish a robust visual foundation, our spatial processing pipeline builds upon the detection architecture of LLMDet [10]. However, to transcend this static perception for dynamic SMOT, we introduce continuous geometric tracking and a novel Spatio-Temporal Fusion Module, effectively transforming independent frame-level detections into coherent video-level narratives. Specifically, we employ Grounding DINO [27] for detection. Similar to transformer trackers that operate without additional queries or networks [24],

we extract detection boxes and visual embeddings in a single forward pass. Subsequently, we utilize Byte [65] to ensure robust data association. The resulting visual features are then compressed by our dual-stream Fusion Module into compact tokens. Finally, to maintain temporal consistency while mitigating the memory bottleneck of LLMs, we introduce a recursive prompting mechanism where the semantic state of the previous frame \mathcal{S}_{t-1} serves as a linguistic prior for the current generation.

4.2 Spatio-Temporal Fusion Module

Directly feeding frame-wise visual tokens into an LLM is computationally prohibitive and introduces temporal redundancy. To bridge the gap between high-frequency visual signals and high-level semantic reasoning, we design a lightweight **Fusion Module**. This module compresses the visual stream into two distinct sets of compact tokens: *Video Context Tokens* and *Instance Dynamic Tokens*.

Video Fusion: Global Context Aggregation. To capture the evolving environmental atmosphere (*e.g.*, weather changes, scene transitions), we employ a recursive update mechanism. Let $f_t^{img} \in \mathbb{R}^{H \times W \times C}$ be the visual features of the current frame. We maintain a running memory token M_{t-1}^{env} representing the global context up to time $t-1$. The current environment token M_t^{env} is updated via a Cross-Attention mechanism where the memory serves as the Query, and the current frame features serve as Key and Value:

$$M_t^{env} = \text{Norm}(M_{t-1}^{env} + \text{Attention}(Q = M_{t-1}^{env}, K = f_t^{img}, V = f_t^{img})) \quad (1)$$

This recurrent formulation allows the model to compress arbitrarily long video sequences into a fixed-size representation, strictly adhering to the online processing constraint.

Instance Fusion: Adaptive Temporal Association. Similarly, for individual objects, modeling actions requires analyzing motion patterns within a relevant timeframe. We apply the same sliding window strategy to object trajectories. For the i -th target at frame t , let $\mathbf{V}_t^i = \{v_k^i\}_{k=\max(0, t-L+1)}^t$ be the sequence of object visual embeddings within the window.

To fuse this sequence into a compact instance token h_t^i , we employ an adaptive additive attention mechanism. We calculate a significance weight α_k for each historical frame k relative to the current state v_t^i :

$$e_k = \mathbf{w}_2^\top \tanh(\mathbf{W}1[v_t^i; v_k^i] + b_1), \quad \alpha_k = \text{Softmax}(e_k) \quad (2)$$

The final instance representation is obtained by the weighted aggregation of the historical features:

$$h_t^i = \text{Linear}\left(\sum k \alpha_k v_k^i\right) \quad (3)$$

By sharing the same window size L across both video and instance modules, LLMTrack maintains a synchronized temporal receptive field, ensuring that the semantic reasoning for both the environment and agents is temporally aligned.

Online Recursive Generation. A core challenge in online semantic tracking is maintaining narrative consistency. We address this by explicitly conditioning the LLM generation on the immediate past and enforcing our *Macro-Understanding-First* paradigm. Crucially, while the Video Context Token (M_t^{env}) provides a stable anchor for the overall scene, the Instance Dynamic Tokens ($\{h_t^i\}$) are optimized to capture fine-grained actions. By structurally preceding the instance tokens with the global token in the prompt, the LLM’s causal self-attention mechanism natively forces the micro-level descriptions to deeply condition on the macro-level context. This prevents hallucinated interactions between agents. We construct the prompt \mathcal{P}_t for the current frame as a concatenation of the task instruction \mathcal{I} , the previous semantic output \mathcal{S}_{t-1} , and the current fused visual tokens:

$$\mathcal{P}_t = [\mathcal{I}; \text{“Previous State:”} \oplus \mathcal{S}_{t-1}; \text{“Current Observation:”} \oplus M_t^{env} \oplus \{h_t^i\}_{i=1}^{N_t}] \quad (4)$$

Crucially, by prepending the global environment token M_t^{env} to the instance tokens $\{h_t^i\}$, the LLM’s causal self-attention natively forces the micro-level instance descriptions to deeply condition on the macro-level context. The model then estimates the probability of the current description \mathcal{S}_t :

$$P(\mathcal{S}_t | \mathcal{V}_t) = \prod_{j=1}^{|\mathcal{S}_t|} P(w_j | w_{<j}, \mathcal{P}_t) \quad (5)$$

By explicitly including \mathcal{S}_{t-1} , the model is encouraged to generate differential descriptions, focusing on *what has changed* relative to the last moment, which significantly stabilizes the output in long-term tracking scenarios.

4.3 Progressive Three-Stage Training

Training a unified architecture for both geometric tracking and semantic reasoning is challenging. To ensure stability and efficiency, we propose a progressive training strategy.

Stage 1: Geometric Warm-up.

In the initial stage, we focus exclusively on establishing a robust geometric foundation by training the visual tracker and the fusion module jointly. Following the design of FastTrackTr, we employ standard tracking losses \mathcal{L}_{track} (including L1 loss [41], GIoU loss [40], focal loss [25], and circle loss [45]). Crucially, the Large Language Model is entirely excluded from this phase. This isolation prevents premature feature distortion that could arise from complex semantic gradients before the tracker achieves reliable spatial localization. To reduce memory overhead and accelerate training, we adopt the sparse frame sampling strategy from

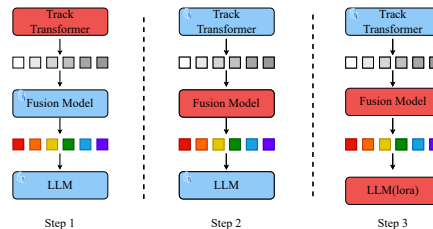


Fig. 4: The progressive three-stage training paradigm. Red indicates trainable components, while blue indicates frozen ones. **Step 1** focuses on tracking. **Step 2** aligns fusion with LLM. **Step 3** fine-tunes LLM via LoRA [15].

the Large Language Model is entirely excluded from this phase. This isolation prevents premature feature distortion that could arise from complex semantic gradients before the tracker achieves reliable spatial localization. To reduce memory overhead and accelerate training, we adopt the sparse frame sampling strategy from

MOTIP [12], where gradients are back-propagated only on a randomly sampled subset of key frames rather than the entire video sequence. The total objective for this stage is purely geometric:

$$\mathcal{L}_{Stage1} = \mathcal{L}_{track} \quad (6)$$

where \mathcal{L}_{track} comprises standard detection and association losses adapted from FastTrackTr [24].

Stage 2: Semantic Alignment via Decoupled TBPTT. Once the tracker converges, we freeze the tracking networks to prevent feature drift, focusing exclusively on optimizing the Fusion Module via a Causal Language Modeling (CLM) objective. Processing long sequences natively exceeds GPU memory and starves instance-level modules of gradients due to sparse, sequence-level annotations. To resolve this, we adopt a **Decoupled Dense-Sparse Optimization** strategy based on Truncated Back-Propagation Through Time (TBPTT) [55,58] (further implementation details are provided in **Appendix**).

We discretize the video into short clips $\mathcal{V} = \{C_1, \dots, C_K\}$. At step k , the Fusion Module initializes its states using the cached outputs from C_{k-1} , applying a **stop-gradient operation** ($\text{sg}(\cdot)$) to bound the backward pass while preserving global history in the forward pass:

$$\mathbf{H}_k^{global}, \{\tilde{\mathbf{f}}_k^i\} = \text{Fusion}(C_k \mid \text{sg}(\mathbf{H}_{k-1}^{global}), \text{sg}(\{\tilde{\mathbf{f}}_{k-1}^i\})) \quad (7)$$

Consequently, we decouple the CLM objective to match the temporal granularity of the annotations:

$$\mathcal{L}_{Stage2}^{(k)} = \begin{cases} \mathcal{L}_{instance}(C_k) & \text{if } k < K \\ \mathcal{L}_{instance}(C_K) + \lambda_{vid}\mathcal{L}_{video}(\mathbf{H}_K^{global}) & \text{if } k = K \end{cases} \quad (8)$$

Here, $\mathcal{L}_{instance}$ acts as a **dense supervisor** computed at every clip to continuously optimize fine-grained trajectory features. Conversely, \mathcal{L}_{video} serves as a **sparse supervisor**, activated exclusively at the final clip K where the environment token \mathbf{H}_K^{global} has fully encapsulated the holistic scene narrative.

Stage 3: Cognitive Fine-tuning via LoRA. In the final stage, we freeze all visual components including the now-aligned Fusion Module and fine-tune the LLM using Low-Rank Adaptation (LoRA). We continue to strictly adhere to the Decoupled TBPTT protocol established in Stage 2. Even though gradients are temporally truncated between consecutive clips, the LLM learns to reason and generate temporally coherent narratives by conditioning on both the accumulated textual history explicitly embedded in the prompts and the stabilized visual tokens. The optimization objective remains the decoupled Causal Language Modeling loss defined in Eq. 8.

5 Experiments

5.1 Settings and Metrics

Datasets and Metrics. We conduct evaluations on the Grand-SMOT benchmark, strictly adhering to the official splits of its constituent sources (TAO [7]

and BenSMOT [22]). To rigorously assess performance across diverse operational domains, we adopt a dataset-specific evaluation protocol. For the TAO subset, which emphasizes open-vocabulary classification, we employ the **TETA** protocol [20] to decompose performance into localization (LocA), association (AssocA), and classification (ClsA). Conversely, for the BenSMOT subset, we report standard HOTA, DetA, AssA, IDF1, MOTA metrics [29, 42] to benchmark geometric tracking consistency against established baselines. Regarding semantic reasoning, we adopt a hybrid evaluation paradigm. While we retain standard N-gram metrics (BLEU [37], METEOR [2], CIDEr [48]) to facilitate direct comparison with prior baselines [22], we argue that rigid lexical matching is insufficient for modern MLLMs. Therefore, inspired by [31], we introduce the **GPT-4o Semantic Score (GPT-S)** (1-5 Likert) to capture logical coherence, temporal consistency, and narrative depth beyond rigid lexical matching. To mitigate LLM evaluation bias and ensure reliability, we validated GPT-S against human judgments, achieving a strong rank correlation (*e.g.*, Spearman’s $\rho = 0.82$). Exact prompts, sampling parameters, and the human-study calibration are detailed in the **Appendix**.

Implementation Details. We instantiate our visual frontend using the Grounding DINO-T architecture [27], which employs a Swin-Transformer-Tiny [28] backbone for hierarchical feature extraction. This is coupled with a BERT-base [9] text encoder for open-vocabulary alignment and a six-layer Transformer Encoder-Decoder for cross-modal fusion. For the cognitive backend, we integrate this perception module with the LLaVA-OneVision [17] and LLaVA-OneVision-1.5 [1], deploying two variants based on Qwen2-VL-0.5B [50] and Qwen3-VL-4B [59] to investigate scaling laws. To facilitate efficient parameter tuning, we apply LoRA with a rank of $r = 64$ to the linear projection layers. The training is executed on a high-performance node equipped with $8 \times$ NVIDIA RTX 5880 Ada GPUs and, for single GPU, batch size is set to 1; this substantial memory capacity enables us to maximize the temporal window size during training, thereby preserving critical long-term context without resorting to aggressive token pruning. All the codes are built based on PyTorch [38]. In the ablation experiment, unless otherwise stated, training and testing were only conducted on the BenSMOT part. The first stage was trained for 12 epochs, while the second and third stages were both trained for 6 epochs.

5.2 Main Results

Tracking. Table 2 evaluates system-level tracking performance. LLMTrack achieves 75.23% HOTA on BenSMOT, surpassing OC-SORT (71.74%). To reflect peak practical capabilities, traditional baselines are evaluated using their officially optimized detectors (*e.g.*, YOLOX), while LLMTrack intrinsically relies on Grounding DINO. This design choice highlights the architectural advantage of our unified open-world pipeline over traditional closed-set systems. For TAO (Open-World Subset), we adopt TETA instead of HOTA to prevent rare-class classification errors from masking association quality under severe long-tail distribu-

tions. The **Appendix** provides TAO HOTA results, discussions on open-world adaptation challenges, and detailed detector configurations.

Table 2: System-level tracking performance on Grand-SMOT. The benchmark includes a **Standard Subset** (BenSMOT [22]) and an **Open-World Subset** (TAO [7]). Best in **red**, second in **blue**. Methods with an asterisk (*) use their officially optimized detectors (Faster R-CNN [40] or YOLOX [13]) to ensure fair evaluation at their peak capacity, whereas LLMTrack utilizes Grounding DINO to demonstrate the unified open-world paradigm.

Method	Grand-SMOT (BenSMOT Split)				Grand-SMOT (TAO Split)			
	HOTA \uparrow	DetA \uparrow	AssA \uparrow	IDF1 \uparrow	TETA \uparrow	LocA \uparrow	AssocA \uparrow	ClsA \uparrow
SORT* [3]	48.81	60.45	39.22	53.51	24.8	48.1	14.3	12.1
DeepSORT* [57]	49.78	61.88	39.81	57.24	26.0	48.4	17.5	12.1
GTR* [67]	65.34	66.21	64.52	72.45	32.5	50.2	35.2	12.1
ByteTrack* [65]	68.21	67.58	70.81	78.85	29.2	49.1	26.8	12.1
OC-SORT* [4]	71.74	69.12	73.81	78.22	27.5	48.5	22.1	12.1
OVTR [18]	68.42	63.52	73.71	71.53	33.2	50.0	34.5	15.1
OVTrack* [21]	69.15	64.18	74.53	72.35	34.7	49.3	36.7	18.1
SMOTer [22]	71.55	71.32	73.28	80.18	-	-	-	-
LLMTrack (Ours)	75.23	73.68	77.52	84.31	33.6	50.6	36.0	14.2

Semantic Understanding. As shown in Table 3, LLMTrack demonstrates a qualitative leap in semantic tasks across both the BenSMOT and TAO splits. Notably, LLMTrack-4B achieves a Video CIDEr of 0.425 and an average GPT-4o Semantic Score (GPT-S) of 3.8 on BenSMOT, evaluating five dimensions (Correctness, Detail, Context, Temporal, and Consistency). This margin highlights that large language models offer vastly superior reasoning for complex social interactions compared to BERT-based architectures. Furthermore, to ensure a fair comparison, we equipped traditional trackers with our exact 0.5B LLM backend and fusion module, extracting object queries from standard bounding-box crops using a Swin-Transformer-Tiny. Despite this, our 0.5B variant consistently prevails, proving that our natively extracted trajectory representations capture far richer spatio-temporal context than these standard crop-based features. Finally, the consistent performance boost from 0.5B to 4B confirms our framework’s strong scalability in translating broader world knowledge into fine-grained video understanding. Detailed baseline configurations and granular dimension-wise GPT-S results are deferred to the **Appendix**.

5.3 Ablation Studies

Experimental Setup for Ablations. To conserve computational resources and ensure a fair comparison, all ablation studies reported in this section were conducted exclusively on the **BenSMOT** dataset and utilize our **LLMTrack-0.5B** model variant. Unless otherwise explicitly stated, the models analyzed here were trained solely on BenSMOT without the inclusion of the TAO dataset.

Table 3: Semantic Understanding performance on Grand-SMOT. To ensure a strictly fair comparison, methods marked with an asterisk (*) utilize the exact same 0.5B LLM backend and fusion module as LLMTrack-0.5B. **GPT-S** denotes the overall GPT-4o Semantic Score (1-5), which is averaged over five fine-grained evaluation dimensions. Detailed dimension-wise results are provided in the **Appendix**.

Method	Grand-SMOT (BenSMOT Split)								Grand-SMOT (TAO Split)							
	Video Caption				Instance Caption				Video Caption				Instance Caption			
	B-4↑	M↑	C↑	GPT-S↑	B-4↑	M↑	C↑	GPT-S↑	B-4↑	M↑	C↑	GPT-S↑	B-4↑	M↑	C↑	GPT-S↑
SORT* [3]	0.115	0.141	0.225	2.7	0.132	0.155	0.250	1.4	0.102	0.130	0.195	2.5	0.118	0.135	0.215	1.5
DeepSORT* [57]	0.122	0.148	0.238	2.8	0.145	0.162	0.265	1.5	0.108	0.135	0.208	2.6	0.125	0.142	0.228	1.6
GTR* [67]	0.135	0.155	0.255	2.9	0.158	0.170	0.285	1.6	0.115	0.142	0.220	2.7	0.138	0.155	0.245	1.7
ByteTrack* [65]	0.142	0.165	0.270	3.0	0.168	0.185	0.305	1.7	0.125	0.150	0.235	2.8	0.145	0.162	0.260	1.8
OC-SORT* [4]	0.148	0.168	0.285	3.1	0.172	0.192	0.320	1.8	0.128	0.152	0.245	2.9	0.148	0.168	0.268	1.9
OVTR [18]	0.160	0.182	0.318	3.2	0.180	0.208	0.348	1.9	0.132	0.166	0.270	3.1	0.158	0.180	0.302	2.0
OVTrack* [21]	0.152	0.178	0.305	3.1	0.184	0.198	0.350	1.9	0.138	0.162	0.278	3.1	0.152	0.176	0.298	2.0
SMOTer [22]	0.045	0.095	0.110	2.1	0.062	0.112	0.145	1.1	-	-	-	-	-	-	-	-
LLMTrack-0.5B (Ours)	0.156	0.185	0.315	3.3	0.182	0.205	0.355	2.0	0.135	0.165	0.275	3.2	0.155	0.182	0.305	2.1
LLMTrack-4B (Ours)	0.198	0.224	0.425	3.8	0.235	0.248	0.485	2.9	0.175	0.198	0.380	3.9	0.195	0.215	0.415	2.8

The impact of various components and datasets. We validated the contribution of each component using the LLMTrack-0.5B model (Table 4). The addition of Grounding DINO (GD) immediately improved HOTA. However, semantic metrics only improved significantly after introducing LoRA. Most importantly, the combination of Instance Fusion (Ins-Fus) and Video Fusion (Vid-Fus) proved essential for capturing interactions (highest mF1) and summarizing the scene (highest Video CIDEr). The initial understanding is to directly use the LLM for zero-shot inference.

Table 4: Ablation study on core components and data scale. We progressively integrate modules and data sources to validate their contributions. **Data:** Training source (Ben: BenSMOT only, +TAO: BenSMOT + TAO); **GD:** Grounding DINO frontend; **LoRA:** Low-Rank Adaptation for LLM; **Vid:** Video Fusion Module; **Ins:** Instance Fusion Module. **GPT-S** denotes the GPT-4o Semantic Score.

Data	Components				Tracking		Video Summary			Instance Desc.		
	GD	LoRA	Vid	Ins	HOTA	IDF1	METEOR	CIDEr	GPT-S	METEOR	CIDEr	GPT-S
Ben	-	-	-	-	72.58	81.68	0.084	0.108	1.9	0.095	0.121	1.1
Ben	✓	-	-	-	74.61	83.52	0.086	0.112	1.9	0.098	0.125	1.1
Ben	✓	✓	-	-	74.61	83.52	0.148	0.236	2.6	0.162	0.248	1.5
Ben	✓	✓	✓	-	74.61	83.52	0.175	0.292	3.0	0.165	0.252	1.5
Ben	✓	✓	✓	✓	74.61	83.52	0.178	0.298	3.1	0.195	0.338	1.9
+TAO	✓	✓	✓	✓	75.23	84.31	0.185	0.315	3.3	0.205	0.355	2.0

Impact of Progressive Training Paradigms. We validate our three-stage pipeline in Table 5. Notably, underlying tracking performance (*e.g.*, HOTA, IDF1) is established early in the training process and remains completely unaffected by these semantic tuning variants; thus, we omit geometric metrics to focus on semantic capabilities. Skipping the Stage 2 alignment drastically degrades generation (CIDEr drops to 0.245), proving that a shared latent space is essential before LLM activation. Furthermore, freezing the Fusion Module during Stage 3 (Row 2) yields suboptimal temporal representations (0.315 CIDEr).

Table 5: Impact of different training paradigms on model convergence and performance. We analyze the contribution of the intermediate alignment stage and the necessity of tuning the fusion module during the final stage. Tracking performance remains consistent across all variants and is omitted for brevity.

Training Strategy	Instance Desc.			Video Summary		
	METEOR \uparrow	CIDEr \uparrow	GPT-S \uparrow	METEOR \uparrow	CIDEr \uparrow	GPT-S \uparrow
Stage 1 \rightarrow Stage 3 (w/o Stage 2)	0.160	0.245	1.5	0.145	0.202	2.4
Stage 1 \rightarrow Stage 2 \rightarrow Stage 3 (w/o Fusion)	0.188	0.320	1.8	0.172	0.285	3.0
Stage 1 \rightarrow Stage 2 \rightarrow Stage 3 (Full)	0.195	0.338	1.9	0.178	0.298	3.1

Jointly fine-tuning it alongside the LLM is therefore crucial for adapting spatio-temporal priors to complex instructions.

Analysis of Fusion Window Size. Table 6 ablates the temporal aggregation window size (L) in the Fusion Module. Since spatial association relies primarily on local motion cues extracted from the frontend, geometric tracking metrics remain entirely invariant to changes in the semantic fusion window size (L) and are therefore not reported here. Semantic understanding, however, requires broader context. A restricted window ($L = 10$) fails to capture complex actions, severely reducing CIDEr. Expanding to $L = 30$ optimally balances context retention and online constraints, achieving results highly competitive with the offline upper bound ($L = \text{Full sequence}$). Thus, we adopt $L = 30$ as our default.

Table 6: Impact of fusion window size (L) during inference. We evaluate how the temporal aggregation range in the Fusion Module affects performance. Evaluated on the BenSMOT split for the 0.5B model. $L = \text{Full}$ serves as an offline upper bound. Note that $L = \text{Full}$ is only feasible on BenSMOT due to its shorter sequence lengths (~ 70 frames); TAO sequences can exceed a thousand frames, making full-sequence offline processing computationally intractable for the LLM.

Window Size (L)	Instance Desc.			Video Summary		
	METEOR \uparrow	CIDEr \uparrow	GPT-S \uparrow	METEOR \uparrow	CIDEr \uparrow	GPT-S \uparrow
$L = 10$ (Short)	0.175	0.284	1.6	0.160	0.256	2.7
$L = 20$ (Medium)	0.188	0.327	1.8	0.171	0.293	3.0
$L = 30$ (Default Online)	0.195	0.338	1.9	0.178	0.298	3.1
$L = \text{Full}$ (Offline Bound)	0.194	0.341	1.9	0.180	0.320	3.4

6 Conclusion

This paper pioneers a semantic paradigm shift in SMOT by introducing Grand-SMOT and LLMTrack. Grand-SMOT innovates with a dual-stream dense description strategy, while LLMTrack establishes a *Macro-Understanding-First* cognitive framework. By aligning geometric trajectories with semantic reasoning via our Spatio-Temporal Fusion Module, we achieve state-of-the-art performance (75.23% HOTA). Looking forward, we aim to leverage Scaling Laws with massive foundation models (30B+) and pursue End-to-End Unification, where high-level semantic feedback directly refines low-level association. Ultimately, we aspire to upgrade LLMTrack from a descriptive tracker into a predictive World Model, shifting focus from passive observation to active forecasting to serve as the cognitive core for next-generation open-world agents.

References

1. An, X., Xie, Y., Yang, K., Zhang, W., Zhao, X., Cheng, Z., Wang, Y., Xu, S., Chen, C., Wu, C., et al.: Llava-onevision-1.5: Fully open framework for democratized multimodal training. arXiv preprint arXiv:2509.23661 (2025) [2](#), [3](#), [4](#), [11](#), [24](#), [35](#), [36](#)
2. Banerjee, S., Lavie, A.: Meteor: An automatic metric for mt evaluation with improved correlation with human judgments. In: Proceedings of the acl workshop on intrinsic and extrinsic evaluation measures for machine translation and/or summarization. pp. 65–72 (2005) [11](#)
3. Bewley, A., Ge, Z., Ott, L., Ramos, F., Upcroft, B.: Simple online and realtime tracking. In: 2016 IEEE International Conference on Image Processing (ICIP). pp. 3464–3468 (Sep 2016) [3](#), [12](#), [13](#), [30](#), [31](#), [32](#), [33](#), [34](#)
4. Cao, J., Pang, J., Weng, X., Khirodkar, R., Kitani, K.: Observation-centric sort: Rethinking sort for robust multi-object tracking. In: Proceedings of the IEEE/CVF Conference on Computer Vision and Pattern Recognition. pp. 9686–9696 (2023) [12](#), [13](#), [30](#), [31](#), [32](#), [33](#), [34](#)
5. Chen, G.H., Chen, S., Zhang, R., Chen, J., Wu, X., Zhang, Z., Chen, Z., Li, J., Wan, X., Wang, B.: Allava: Harnessing gpt4v-synthesized data for lite vision-language models. arXiv preprint arXiv:2402.11684 (2024) [3](#)
6. Chen, L., Li, J., Dong, X., Zhang, P., He, C., Wang, J., Zhao, F., Lin, D.: Sharegpt4v: Improving large multi-modal models with better captions. In: European Conference on Computer Vision. pp. 370–387. Springer (2024) [2](#), [3](#), [4](#)
7. Dave, A., Khurana, T., Tokmakov, P., Schmid, C., Ramanan, D.: Tao: A large-scale benchmark for tracking any object. In: European conference on computer vision. pp. 436–454. Springer (2020) [2](#), [4](#), [5](#), [6](#), [10](#), [12](#)
8. Dendorfer, P., Rezatofighi, H., Milan, A., Shi, J., Cremers, D., Reid, I., Roth, S., Schindler, K., Leal-Taixé, L.: Mot20: A benchmark for multi object tracking in crowded scenes. arXiv preprint arXiv:2003.09003 (2020) [6](#)
9. Devlin, J., Chang, M.W., Lee, K., Toutanova, K.: Bert: Pre-training of deep bidirectional transformers for language understanding. arXiv preprint arXiv:1810.04805 (2018) [4](#), [11](#)
10. Fu, S., Yang, Q., Mo, Q., Yan, J., Wei, X., Meng, J., Xie, X., Zheng, W.S.: Llm-det: Learning strong open-vocabulary object detectors under the supervision of large language models. In: Proceedings of the Computer Vision and Pattern Recognition Conference. pp. 14987–14997 (2025) [4](#), [7](#)
11. Gadre, S.Y., Ilharco, G., Fang, A., Hayase, J., Smyrnis, G., Nguyen, T., Marten, R., Wortsman, M., Ghosh, D., Zhang, J., et al.: Datacomp: In search of the next generation of multimodal datasets. Advances in Neural Information Processing Systems **36**, 27092–27112 (2023) [2](#)
12. Gao, R., Qi, J., Wang, L.: Multiple object tracking as id prediction. In: Proceedings of the Computer Vision and Pattern Recognition Conference. pp. 27883–27893 (2025) [1](#), [3](#), [10](#), [25](#)
13. Ge, Z.: Yolox: Exceeding yolo series in 2021. arXiv preprint arXiv:2107.08430 (2021) [12](#)
14. Gupta, A., Dollar, P., Girshick, R.: Lvis: A dataset for large vocabulary instance segmentation. In: Proceedings of the IEEE/CVF conference on computer vision and pattern recognition. pp. 5356–5364 (2019) [4](#)
15. Hu, E.J., Shen, Y., Wallis, P., Allen-Zhu, Z., Li, Y., Wang, S., Wang, L., Chen, W., et al.: Lora: Low-rank adaptation of large language models. In: ICLR. vol. 1, p. 3 (2022) [9](#)

16. Kaplan, J., McCandlish, S., Henighan, T., Brown, T.B., Chess, B., Child, R., Gray, S., Radford, A., Wu, J., Amodei, D.: Scaling laws for neural language models. arXiv preprint arXiv:2001.08361 (2020) [2](#)
17. Li, B., Zhang, Y., Guo, D., Zhang, R., Li, F., Zhang, H., Zhang, K., Zhang, P., Li, Y., Liu, Z., et al.: Llava-onevision: Easy visual task transfer. arXiv preprint arXiv:2408.03326 (2024) [2](#), [3](#), [4](#), [11](#), [24](#), [35](#), [36](#)
18. Li, J., Yu, E., Chen, S., Tao, W.: Ovtr: End-to-end open-vocabulary multiple object tracking with transformer. arXiv preprint arXiv:2503.10616 (2025) [12](#), [13](#), [31](#), [34](#)
19. Li, K., He, Y., Wang, Y., Li, Y., Wang, W., Luo, P., Wang, Y., Wang, L., Qiao, Y.: Videochat: Chat-centric video understanding. *Science China Information Sciences* **68**(10), 200102 (2025) [4](#)
20. Li, S., Danelljan, M., Ding, H., Huang, T.E., Yu, F.: Tracking every thing in the wild. In: European conference on computer vision. pp. 498–515. Springer (2022) [11](#)
21. Li, S., Fischer, T., Ke, L., Ding, H., Danelljan, M., Yu, F.: Ovtrack: Open-vocabulary multiple object tracking. In: Proceedings of the IEEE/CVF conference on computer vision and pattern recognition. pp. 5567–5577 (2023) [12](#), [13](#), [30](#), [31](#), [34](#)
22. Li, Y., Li, Q., Wang, H., Ma, X., Yao, J., Dong, S., Fan, H., Zhang, L.: Beyond mot: Semantic multi-object tracking. In: European Conference on Computer Vision. pp. 276–293. Springer (2024) [1](#), [2](#), [4](#), [5](#), [6](#), [11](#), [12](#), [13](#), [24](#), [32](#), [33](#), [34](#)
23. Liao, P., Yang, F., Wu, D., Yu, J., Li, X., Zhang, D.: Fasttracktr: Real-time multi-object tracking with transformers for real world. *IEEE Transactions on Industrial Informatics* pp. 1–11 (2025) [1](#)
24. Liao, P., Yang, F., Wu, D., Yu, J., Li, X., Zhang, D.: Fasttracktr: Real-time multi-object tracking with transformers for real world. *IEEE Transactions on Industrial Informatics* (2025) [7](#), [10](#)
25. Lin, T.Y., Goyal, P., Girshick, R., He, K., Dollár, P.: Focal loss for dense object detection. In: Proceedings of the IEEE international conference on computer vision. pp. 2980–2988 (2017) [9](#)
26. Liu, H., Li, C., Li, Y., Lee, Y.J.: Improved baselines with visual instruction tuning. In: Proceedings of the IEEE/CVF conference on computer vision and pattern recognition. pp. 26296–26306 (2024) [4](#)
27. Liu, S., Zeng, Z., Ren, T., Li, F., Zhang, H., Yang, J., Jiang, Q., Li, C., Yang, J., Su, H., et al.: Grounding dino: Marrying dino with grounded pre-training for open-set object detection. In: European conference on computer vision. pp. 38–55. Springer (2024) [3](#), [7](#), [11](#), [26](#), [31](#)
28. Liu, Z., Lin, Y., Cao, Y., Hu, H., Wei, Y., Zhang, Z., Lin, S., Guo, B.: Swin transformer: Hierarchical vision transformer using shifted windows. In: Proceedings of the IEEE/CVF international conference on computer vision. pp. 10012–10022 (2021) [11](#)
29. Luiten, J., Osep, A., Dendorfer, P., Torr, P., Geiger, A., Leal-Taixé, L., Leibe, B.: Hota: A higher order metric for evaluating multi-object tracking. *International journal of computer vision* **129**, 548–578 (2021) [11](#)
30. Lv, W., Zhang, N., Sun, H., Jiang, H., Zhao, K., Xiao, J., Zeng, D.: Vision-motion-reference alignment for referring multi-object tracking via multi-modal large language models. arXiv preprint arXiv:2511.17681 (2025) [1](#), [4](#)
31. Maaz, M., Rasheed, H., Khan, S., Khan, F.: Video-chatgpt: Towards detailed video understanding via large vision and language models. In: Proceedings of the 62nd Annual Meeting of the Association for Computational Linguistics (Volume 1: Long Papers). pp. 12585–12602 (2024) [11](#), [32](#)

32. Maggolino, G., Ahmad, A., Cao, J., Kitani, K.: Deep oc-sort: Multi-pedestrian tracking by adaptive re-identification. In: 2023 IEEE International conference on image processing (ICIP). pp. 3025–3029. IEEE (2023) [1](#), [4](#)
33. Meinhardt, T., Kirillov, A., Leal-Taixe, L., Feichtenhofer, C.: Trackformer: Multi-object tracking with transformers. In: Proceedings of the IEEE/CVF conference on computer vision and pattern recognition. pp. 8844–8854 (2022) [3](#)
34. Milan, A., Leal-Taixe, L., Reid, I., Roth, S., Schindler, K.: MOT16: A Benchmark for Multi-Object Tracking (May 2016) [6](#)
35. Nguyen, P., Quach, K.G., Kitani, K., Luu, K.: Type-to-track: Retrieve any object via prompt-based tracking. Advances in Neural Information Processing Systems **36**, 3205–3219 (2023) [6](#)
36. Pang, J., Qiu, L., Li, X., Chen, H., Li, Q., Darrell, T., Yu, F.: Quasi-dense similarity learning for multiple object tracking. In: Proceedings of the IEEE/CVF conference on computer vision and pattern recognition. pp. 164–173 (2021) [3](#)
37. Papineni, K., Roukos, S., Ward, T., Zhu, W.J.: Bleu: a method for automatic evaluation of machine translation. In: Proceedings of the 40th annual meeting of the Association for Computational Linguistics. pp. 311–318 (2002) [11](#)
38. Paszke, A., Gross, S., Massa, F., Lerer, A., Bradbury, J., Chanan, G., Killeen, T., Lin, Z., Gimelshein, N., Antiga, L., et al.: Pytorch: An imperative style, high-performance deep learning library. Advances in neural information processing systems **32** (2019) [11](#)
39. Raja, R., Vats, A., Thawakar, O., Ashraf, T.: Object tracking: A comprehensive survey from classical approaches to large vision-language and foundation models. Available at SSRN 5541079 (2025) [1](#)
40. Ren, S., He, K., Girshick, R., Sun, J.: Faster r-cnn: Towards real-time object detection with region proposal networks. IEEE transactions on pattern analysis and machine intelligence **39**(6), 1137–1149 (2016) [9](#), [12](#)
41. Rezatofighi, H., Tsoi, N., Gwak, J., Sadeghian, A., Reid, I., Savarese, S.: Generalized intersection over union: A metric and a loss for bounding box regression. In: Proceedings of the IEEE/CVF conference on computer vision and pattern recognition. pp. 658–666 (2019) [9](#)
42. Ristani, E., Solera, F., Zou, R., Cucchiara, R., Tomasi, C.: Performance measures and a data set for multi-target, multi-camera tracking. In: European conference on computer vision. pp. 17–35. Springer (2016) [11](#)
43. Sun, P., Cao, J., Jiang, Y., Yuan, Z., Bai, S., Kitani, K., Luo, P.: DanceTrack: Multi-Object Tracking in Uniform Appearance and Diverse Motion. In: 2022 IEEE/CVF Conference on Computer Vision and Pattern Recognition (CVPR). pp. 20961–20970. IEEE, New Orleans, LA, USA (Jun 2022) [6](#)
44. Sun, P., Cao, J., Jiang, Y., Zhang, R., Xie, E., Yuan, Z., Wang, C., Luo, P.: Transtrack: Multiple object tracking with transformer. arXiv preprint arXiv:2012.15460 (2020) [24](#), [30](#), [32](#), [33](#)
45. Sun, Y., Cheng, C., Zhang, Y., Zhang, C., Zheng, L., Wang, Z., Wei, Y.: Circle loss: A unified perspective of pair similarity optimization. In: Proceedings of the IEEE/CVF conference on computer vision and pattern recognition. pp. 6398–6407 (2020) [9](#)
46. Team, G., Georgiev, P., Lei, V.I., Burnell, R., Bai, L., Gulati, A., Tanzer, G., Vincent, D., Pan, Z., Wang, S., et al.: Gemini 1.5: Unlocking multimodal understanding across millions of tokens of context. arXiv preprint arXiv:2403.05530 (2024) [2](#), [4](#), [33](#)

47. Team, M., Xiao, C., Li, Y., Han, X., Bai, Y., Cai, J., Chen, H., Chen, W., Cong, X., Cui, G., et al.: Minicpm4: Ultra-efficient llms on end devices. arXiv preprint arXiv:2506.07900 (2025) [6](#), [35](#), [36](#)
48. Vedantam, R., Lawrence Zitnick, C., Parikh, D.: Cider: Consensus-based image description evaluation. In: Proceedings of the IEEE conference on computer vision and pattern recognition. pp. 4566–4575 (2015) [11](#)
49. Wang, N., Zhu, G., Li, H., Zhang, L., Shah, S.A.A., Bennamoun, M.: Language model guided interpretable video action reasoning. In: Proceedings of the IEEE/CVF Conference on Computer Vision and Pattern Recognition. pp. 18878–18887 (2024) [1](#), [4](#)
50. Wang, P., Bai, S., Tan, S., Wang, S., Fan, Z., Bai, J., Chen, K., Liu, X., Wang, J., Ge, W., et al.: Qwen2-vl: Enhancing vision-language model’s perception of the world at any resolution. arXiv preprint arXiv:2409.12191 (2024) [2](#), [11](#), [35](#), [36](#)
51. Wang, Q., Chen, S., Shen, Y.: Causalvtg: Towards robust video temporal grounding via causal inference. In: The Thirty-ninth Annual Conference on Neural Information Processing Systems [2](#)
52. Wang, W., Gao, Z., Gu, L., Pu, H., Cui, L., Wei, X., Liu, Z., Jing, L., Ye, S., Shao, J., et al.: Internvl3.5: Advancing open-source multimodal models in versatility, reasoning, and efficiency. arXiv preprint arXiv:2508.18265 (2025) [35](#), [36](#)
53. Wang, Z., Zheng, L., Liu, Y., Li, Y., Wang, S.: Towards real-time multi-object tracking. In: European conference on computer vision. pp. 107–122. Springer (2020) [7](#)
54. Wei, J., Tay, Y., Bommasani, R., Raffel, C., Zoph, B., Borgeaud, S., Yogatama, D., Bosma, M., Zhou, D., Metzler, D., et al.: Emergent abilities of large language models. arXiv preprint arXiv:2206.07682 (2022) [2](#)
55. Weng, Y., Han, M., He, H., Chang, X., Zhuang, B.: Longvlm: Efficient long video understanding via large language models. In: European Conference on Computer Vision. pp. 453–470. Springer (2024) [10](#)
56. Williams, R.J., Zipser, D.: A learning algorithm for continually running fully recurrent neural networks. *Neural computation* **1**(2), 270–280 (1989) [26](#)
57. Wojke, N., Bewley, A., Paulus, D.: Simple online and realtime tracking with a deep association metric. In: 2017 IEEE international conference on image processing (ICIP). pp. 3645–3649. IEEE (2017) [3](#), [12](#), [13](#), [24](#), [30](#), [31](#), [32](#), [33](#), [34](#)
58. Wu, C.Y., Li, Y., Mangalam, K., Fan, H., Xiong, B., Malik, J., Feichtenhofer, C.: Memvit: Memory-augmented multiscale vision transformer for efficient long-term video recognition. In: Proceedings of the IEEE/CVF conference on computer vision and pattern recognition. pp. 13587–13597 (2022) [10](#)
59. Yang, A., Li, A., Yang, B., Zhang, B., Hui, B., Zheng, B., Yu, B., Gao, C., Huang, C., Lv, C., et al.: Qwen3 technical report. arXiv preprint arXiv:2505.09388 (2025) [2](#), [3](#), [5](#), [11](#), [35](#), [36](#)
60. Yang, J., Dong, Y., Liu, S., Li, B., Wang, Z., Tan, H., Jiang, C., Kang, J., Zhang, Y., Zhou, K., et al.: Octopus: Embodied vision-language programmer from environmental feedback. In: European conference on computer vision. pp. 20–38. Springer (2024) [1](#)
61. Yin, W., Cai, Z., Wang, R., Wang, F., Wei, C., Mei, H., Xiao, W., Yang, Z., Sun, Q., Yamashita, A., et al.: Whac: World-grounded humans and cameras. In: European Conference on Computer Vision. pp. 20–37. Springer (2024) [1](#)
62. Zeng, A., Lv, X., Hou, Z., Du, Z., Zheng, Q., Chen, B., Yin, D., Ge, C., Xie, C., Wang, C., et al.: Glm-5: from vibe coding to agentic engineering. arXiv preprint arXiv:2602.15763 (2026) [33](#)

63. Zeng, F., Dong, B., Zhang, Y., Wang, T., Zhang, X., Wei, Y.: Motr: End-to-end multiple-object tracking with transformer. In: European Conference on Computer Vision. pp. 659–675. Springer (2022) [1](#), [3](#), [30](#), [32](#), [33](#)
64. Zhang, S., Hao, X., Tang, Y., Zhang, L., Wang, P., Wang, Z., Ma, H., Zhang, S.: Video-cot: A comprehensive dataset for spatiotemporal understanding of videos based on chain-of-thought. In: Proceedings of the 33rd ACM International Conference on Multimedia. pp. 12745–12752 (2025) [2](#), [4](#)
65. Zhang, Y., Sun, P., Jiang, Y., Yu, D., Weng, F., Yuan, Z., Luo, P., Liu, W., Wang, X.: Bytetrack: Multi-object tracking by associating every detection box. In: European conference on computer vision. pp. 1–21. Springer (2022) [1](#), [3](#), [8](#), [12](#), [13](#), [24](#), [30](#), [31](#), [32](#), [33](#), [34](#)
66. Zhang, Y., Zhao, J., Nie, S., Kuang, J., Wang, S.: Epiptack: Rethinking prompt modeling with explicit and implicit prompts for multi-object tracking. arXiv preprint arXiv:2510.13235 (2025) [1](#), [4](#)
67. Zhou, X., Yin, T., Koltun, V., Krähenbühl, P.: Global tracking transformers. In: Proceedings of the IEEE/CVF Conference on Computer Vision and Pattern Recognition. pp. 8771–8780 (2022) [12](#), [13](#), [31](#), [34](#)

Appendix of LLMTrack

A	Explicit Interaction Modeling and Emergent Deduction	20
A.1	Baseline Architecture: Explicit Feature Fusion	21
A.2	Paradigm Shift: Zero-Shot Text-Only Deduction	23
A.3	Experimental Settings, Results and Discussion	23
B	Training Details	25
B.1	Stage 1: Sparse Frame Sampling for Geometric Warm-up	25
B.2	Stage 2 & 3: Decoupled TBPTT and Memory Caching	26
B.3	Teacher Forcing for Semantic Stability	27
B.4	Analysis of Training Efficiency and Effectiveness	27
C	Grand-SMOT Dataset Statistics	28
D	Additional Results on Grand-SMOT and Adaptation of other Trackers	29
D.1	Adaptation of other Trackers	30
D.2	Tracking Performance on TAO Split	31
D.3	Semantic Understanding Performance on BenSMOT	31
D.4	Granular Dimension-wise Committee Evaluation	32
E	Details of Dataset Annotation	35
E.1	Comprehensive Evaluation of MLLMs for Narrative Generation	35
E.2	Quality Assurance and Multi-Dimensional GPT Evaluation	36
E.3	Quality Assurance and Human-in-the-Loop Verification	36
F	Qualitative Visualizations	37
G	Limitations and Decoupled Evaluation Strategy	41
G.1	Inherent Limitations of Tracking-Dependent Understanding	41
G.2	Decoupled Evaluation for Semantic Understanding	41
H	Prompt Engineering Details	43
H.1	Prompts for Tracking and Inference	43
H.2	Prompts for Dataset Generation and Extension	44
H.3	Prompts for Datasets Evaluation	48
H.4	Prompts for Fine-grained GPT-4o Evaluation	49

A Explicit Interaction Modeling and Emergent Deduction

As posited in the Introduction, a core philosophy of our work is that multi-object “*interaction*” should not be treated as an isolated visual recognition task, but rather as a natural logical deduction that emerges from the interplay between individual dynamic behaviors and the macroscopic environmental context. To empirically validate this hypothesis, we initially designed an explicit interaction-level feature fusion branch as a baseline, and subsequently compared it against a zero-shot, text-only deduction paradigm.

A.1 Baseline Architecture: Explicit Feature Fusion

Figure 5 illustrates the detailed architecture of our early Fusion Module design, alongside its integration with the Large Language Model (LLM). The framework explicitly models instance, interaction, and video contexts, serving to extract robust representations and effectively align multi-modal features.

The Fusion Module first employs a Track-wise Self-Attention mechanism to process variable-length trajectory features, denoted as f_i^1 and f_i^2 for two targets. Specifically, for a trajectory sequence f_i^k , the attention weights α_i^k are computed via sequential linear projections and a tanh activation, normalized by a Softmax function:

$$\alpha_i^k = \text{Softmax}(W_2 \tanh(W_1 f_i^k + b_1) + b_2) \quad (9)$$

where W_1, W_2, b_1 , and b_2 are learnable parameters. This computes a weighted sum of the trajectory sequence, effectively filtering out noisy frames and aggregating critical temporal dynamics into a fixed-length instance representation \tilde{f}_i^k :

$$\tilde{f}_i^k = \sum_t \alpha_{i,t}^k f_{i,t}^k \quad (10)$$

Following the Instance Fusion phase, trajectory features are merged in pairs to capture interpersonal relationships. This is achieved by concatenating the refined features of two targets and passing them through a Multi-Layer Perceptron (MLP) to yield the fused interaction trajectory feature F_{inter} :

$$F_{\text{inter}} = \text{MLP}([\tilde{f}_i^1; \tilde{f}_i^2]) \quad (11)$$

Concurrently, the Video Fusion module aggregates global contextual information. As illustrated in the diagram, it applies Multi-Head Attention (MHA) utilizing the current frame feature f_t^{img} as the query (Q), and the historical environment feature M_{t-1}^{env} as the key and value (K, V). This is followed by a residual connection from the current frame feature and Layer Normalization (Norm):

$$M_t^{\text{env}} = \text{Norm}(f_t^{\text{img}} + \text{MHA}(f_t^{\text{img}}, M_{t-1}^{\text{env}}, M_{t-1}^{\text{env}})) \quad (12)$$

After the Fusion Module, these hierarchical representations—spanning instance-level, interaction-level, and video-level—are tokenized and fed into the LLM. They are initially processed by a shared Self-Attention layer to establish global context across all inputs. To further align the multi-modal streams and ground interactions within the scene, Cross-Attention (CA) mechanisms are applied. Notably, the interaction-level token acts as the query to attend to the video-level token, which provides the key and value. This alignment can be formulated as:

$$H_{\text{inter}}^{\text{out}} = \text{CA}(Q = H_{\text{inter}}, K = H_{\text{vid}}, V = H_{\text{vid}}) \quad (13)$$

where H_{inter} and H_{vid} denote the interaction and video tokens after the initial self-attention, respectively. Finally, all refined tokens are passed through Feed-Forward Networks (FFN) alongside text tokens to generate the comprehensive semantic interaction outputs.

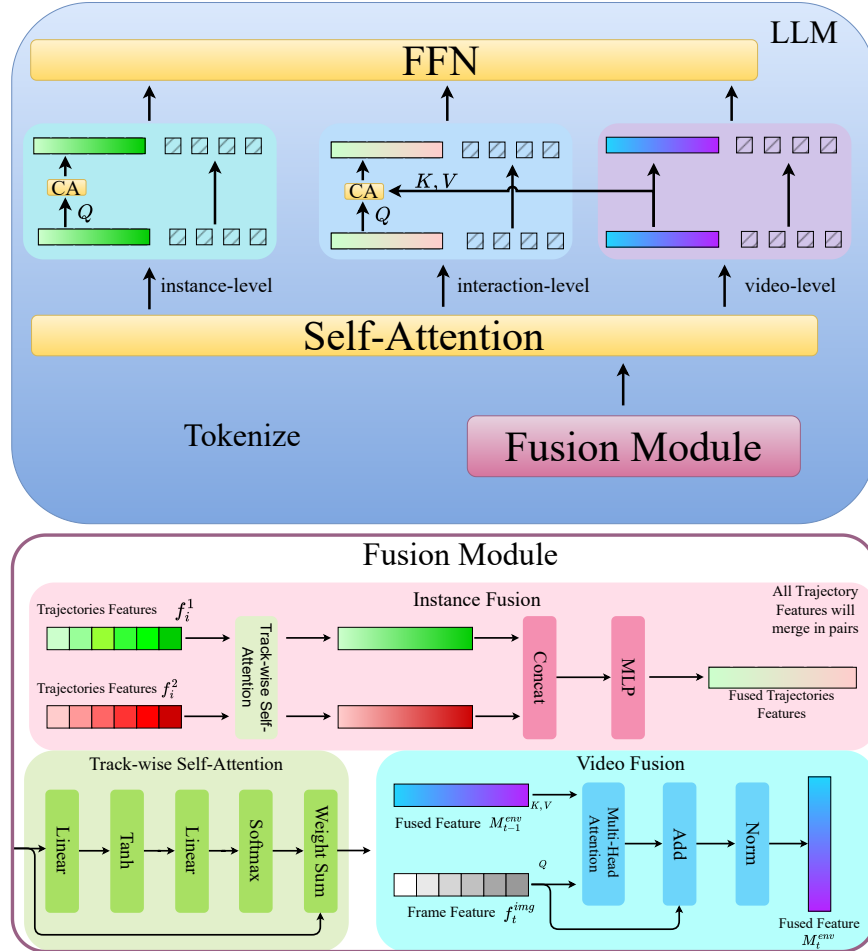


Fig. 5: The detailed architecture of our early explicit feature fusion design. The bottom panel illustrates the hierarchical extraction of instance-level trajectories, explicitly fused interaction-level features (via concatenation and MLP), and video-level contextual embeddings. The top panel details the subsequent integration within the LLM: tokenized multi-modal features first undergo global Self-Attention, followed by a dedicated Cross-Attention (CA) mechanism that meticulously aligns the interaction tokens (as Query) with the video tokens (as Key and Value) prior to the Feed-Forward Networks (FFN). This complex architectural exploration serves as the explicit visual modeling baseline compared against our zero-shot text deduction paradigm.

A.2 Paradigm Shift: Zero-Shot Text-Only Deduction

While traditional paradigms go to great lengths to meticulously design and train explicit feature fusion modules (such as the visual trajectory concatenation and MLP mapping described above) to predict interactions, we hypothesize that such elaborate architectural engineering is often sub-optimal and semantically redundant. If a model possesses sufficient macro-understanding and micro-tracking capabilities, complex social interactions should naturally emerge from the textual narrative.

To verify this and to demonstrate that painstakingly training a dedicated visual interaction branch is less effective than directly leveraging an LLM’s inherent reasoning we designed a zero-shot text-only deduction experiment. In this setting, we entirely discard the visual interaction features and rely exclusively on the pure logical reasoning capabilities of an un-finetuned Large Language Model. Specifically, we utilize the off-the-shelf LLaVA-OneVision and LLaVA-OneVision-1.5 models (0.5B and 4B versions). Let T_{env} denote the video-level environmental summary, and T_A, T_B denote the detailed individual dynamic descriptions of Target A and Target B. The prompt P is formulated by concatenating these text sequences with a task instruction I_{task} :

$$P = \text{Concat}(I_{\text{task}}, T_{\text{env}}, T_A, T_B) \quad (14)$$

The frozen language model, denoted as \mathcal{M}_θ , is then prompted to generate the predicted interaction category \hat{Y}_{inter} purely through text-based logical deduction without any task-specific training:

$$\hat{Y}_{\text{inter}} = \mathcal{M}_\theta(P) \quad (15)$$

A.3 Experimental Settings, Results and Discussion

To comprehensively evaluate the potential and practical robustness of this emergent deduction, we conduct the experiment under two distinct settings. The first setting is Deduction with Ground Truth (GT) Text, where the LLM relies on human-annotated video and instance captions. This serves as a theoretical upper bound to verify information sufficiency, proving that high-quality descriptions of the environment and individuals encapsulate all necessary information entropy required to deduce complex social interactions. The second setting is Deduction with Predicted (Pred) Text, which inputs the actual video summaries and instance narratives generated online by our LLMTrack framework. This setting rigorously assesses the semantic fidelity and causal consistency of our proposed “Macro-Understanding-First” paradigm in practical scenarios.

The performance is evaluated using standard classification metrics, formulated as follows:

$$\text{Precision} = \frac{TP}{TP + FP}, \quad \text{Recall} = \frac{TP}{TP + FN}, \quad F1 = \frac{2 \times \text{Precision} \times \text{Recall}}{\text{Precision} + \text{Recall}} \quad (16)$$

Table 7: Performance comparison between explicit feature fusion and text-only deduction on the interaction recognition task. Representative prior tracking methods, cascaded with the frozen SMOTer text generator, are included to highlight the superiority of the LLM-driven paradigm.

Reasoning Paradigm	Model / Information Source	Precision ↑	Recall ↑	F1 ↑
<i>Previous Methods</i>	DeepSORT [57] + SMOTer Captioner	0.365	0.277	0.310
	ByteTrack [65] + SMOTer Captioner	0.443	0.258	0.326
	TransTrack [44] + SMOTer Captioner	0.406	0.311	0.376
	SMOTer [22]	0.434	0.320	0.368
<i>Baseline: Explicit Feature Fusion</i>	LLMTrack-0.5B + MLP	0.516	0.476	0.496
	LLMTrack-4B + MLP	0.543	0.516	0.526
Text Deduction (w/ Pred Text)	LLaVA-OneVision-0.5B [17] / Generated	0.492	0.468	0.480
Text Deduction (w/ Pred Text)	LLaVA-OneVision-1.5-4B [1] / Generated	0.528	0.502	0.515
Text Deduction (w/ GT Text)	LLaVA-OneVision-0.5B [17] / GT	0.522	0.495	0.508
Text Deduction (w/ GT Text)	LLaVA-OneVision-1.5-4B [1] / GT	0.536	0.548	0.542

where TP , FP , and FN represent the number of True Positives, False Positives, and False Negatives, respectively.

As demonstrated in Table 7, the zero-shot deduction based on Ground Truth text achieves highly compelling performance across both model scales. Notably, all variants of our LLMTrack—whether utilizing explicit feature fusion or pure text deduction—drastically outperform previous cascaded pipelines. The traditional paradigms relying on external frozen captioners struggle with severe error propagation and semantic disjointedness, resulting in sub-optimal F1 scores (e.g., 0.326 for ByteTrack and 0.368 for SMOTer).

More importantly, comparing within our own framework, the zero-shot deductive reasoning consistently rivals or surpasses the explicitly trained fusion modules. Despite the extensive training and architectural complexity required for the LLMTrack-4B explicit feature fusion baseline, it is noticeably outperformed by the completely un-finetuned LLaVA-OneVision-1.5-4B model (with GT Text) in Recall and overall F1 score (0.542 vs. 0.526). A similar trend is observed at the 0.5B scale, where the GT text deduction achieves a higher F1 score (0.508) than its explicitly trained counterpart (0.496). This provides strong empirical evidence that complex social interactions can be more effectively deconstructed as a logical deduction from individual behaviors and environmental contexts, rather than relying on black-box visual feature modeling.

Furthermore, even when relying entirely on the dynamically generated text from our framework (Deduction w/ Pred Text), the models maintain robust performance. The 4B model achieves a competitive F1 score of 0.515 without any task-specific interaction training, which completely eclipses all previous methods. This strongly confirms that our Spatio-Temporal Fusion Module produces dense, causally consistent narratives that are exceptionally reliable for downstream reasoning. Ultimately, these results justify our critical architectural decision to discard the cumbersome explicit interaction branch: laboriously training dedicated modules is demonstrably less effective and less elegant than directly prompting a sufficiently capable LLM to reason over comprehended text.

B Training Details

In this section, we detail the specific training protocols of our framework. Training on long-term video benchmarks (e.g., TAO) presents significant memory challenges. To manage this, we adopt established efficiency protocols tailored to each training stage: sparse frame sampling for the tracker (Stage 1) and sequential clip training with memory caching for the fusion module (Stage 2 & 3).

B.1 Stage 1: Sparse Frame Sampling for Geometric Warm-up

For the initial geometric tracking stage, full temporal back-propagation is impractical due to the massive scale of the visual backbone. Following the protocol in MOTIP [12], we utilize a sparse frame sampling strategy (Fig. 6).

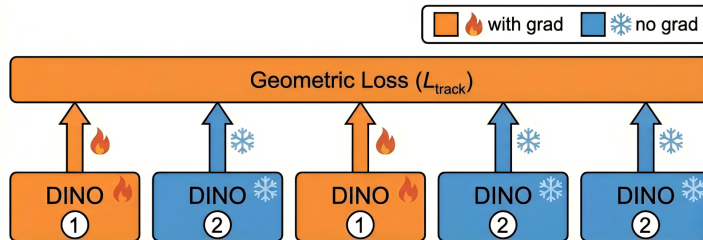


Fig. 6: Illustration of the sparse frame sampling strategy during the initial geometric tracking stage. To mitigate the computational overhead of full temporal back-propagation, gradients are only computed for a sparse subset of sampled frames (orange blocks with fire icons), while the remaining frames only perform forward passes without gradient tracking (blue blocks with snowflake icons).

Crucially, as established in our methodology, this stage is strictly isolated from semantic reasoning to prevent early feature distortion. Gradients are computed only on a randomly sampled subset of key frames $\mathcal{K} = \{t_1, t_2, \dots, t_N\}$ ($N \ll T$). Intermediate frames are processed in inference mode (`no_grad`) to maintain the temporal continuity required for motion estimation, but they do not contribute to the computation graph. The objective is purely geometric:

$$\mathcal{L}_{Stage1} = \frac{1}{|\mathcal{K}|} \sum_{t \in \mathcal{K}} \mathcal{L}_{track}^{(t)} \quad (17)$$

This approach decouples memory usage from the video length, reducing complexity from $\mathcal{O}(T)$ to $\mathcal{O}(N)$ while establishing robust trajectory embeddings. In this paper, N is 4 and T is 30.

B.2 Stage 2 & 3: Decoupled TBPTT and Memory Caching

In Stages 2 and 3, we freeze the visual backbone and transition to long-term semantic alignment. To optimize the Fusion Module and fine-tune the LLM across extended sequences without exceeding hardware limits, we implement the **Decoupled Dense-Sparse Optimization** via Truncated Back-Propagation Through Time (TBPTT) [56].

The video V is partitioned into non-overlapping training clips $\{C_1, C_2, \dots, C_M\}$. To strictly preserve the global context and adhere to our recursive update mechanism, a memory cache \mathcal{M} (containing the environment token \mathbf{H}^{global} and instance states) is passed sequentially from C_{k-1} to C_k :

$$\text{Output}_k, \mathcal{M}_k = \text{Model}(C_k \mid \text{SG}(\mathcal{M}_{k-1})) \quad (18)$$

Here, $\text{SG}(\cdot)$ denotes the stop-gradient operation. This explicitly detaches the historical states from the current computation graph. Consequently, the forward pass continues to perceive the accumulated video history—ensuring long-term narrative consistency while the backward pass is strictly bounded to the local clip size. This mechanism keeps GPU memory usage constant ($\mathcal{O}(L)$) regardless of the total video duration and facilitates the decoupled dense-sparse loss application.

Handling Sparse Annotations in Long Sequences. A unique challenge when training the semantic reasoning modules on benchmarks like TAO is the sparsity of annotations, where ground-truth bounding boxes are sparsely sampled across the temporal dimension. To establish query-to-ground-truth mappings for unannotated frames, we employ a mathematically rigorous extrapolation strategy that decouples spatial association from the disappearance mechanism.

Let t denote the index of the current frame and $\tau = \arg \min_{t' \in \mathcal{T}_{GT}} |t - t'|$ denote the nearest annotated frame, where \mathcal{T}_{GT} is the set of frames containing valid ground-truth annotations. At frame t , a set of tracked queries $Q_t = \{q_t^i\}$ yields predicted bounding boxes $B_t = \{b_t^i\}$ and corresponding semantic grounding scores $S_t = \{s_t^i\}$ (formulated similarly to Grounding DINO [27]). Given the ground-truth boxes $\hat{B}_\tau = \{\hat{b}_\tau^j\}$ at the nearest frame τ , the target assignment y_t^i for each query q_t^i is defined as:

$$y_t^i = \begin{cases} \arg \max_j \text{IoU}(b_t^i, \hat{b}_\tau^j), & \text{if } s_t^i \geq \theta_{score} \text{ and } \max_j \text{IoU}(b_t^i, \hat{b}_\tau^j) \geq \theta_{IoU} \\ \emptyset, & \text{otherwise} \end{cases} \quad (19)$$

where θ_{IoU} is the spatial overlap threshold and θ_{score} is the confidence threshold. The condition $s_t^i < \theta_{score}$ explicitly governs the *disappearance mechanism*: if the grounding confidence of a query falls below θ_{score} , it is immediately assigned to the null state (\emptyset). This effectively models scenarios where the object has visually disappeared, become fully occluded, or exited the field of view. Conversely, if $s_t^i \geq \theta_{score}$ but the IoU remains below θ_{IoU} , it indicates tracking drift, and the query is similarly nullified to prevent binding to an incorrect semantic identity.

Crucially, while all frames undergo a forward pass—utilizing these extrapolated assignments to maintain temporal continuity and update the memory cache \mathcal{M} —the semantic loss computation and back-propagation are strictly restricted to the valid annotated frames ($t \in \mathcal{T}_{GT}$). By masking the loss for frames where $t \notin \mathcal{T}_{GT}$, we effectively prevent noisy gradients caused by extrapolated targets from corrupting the LLM’s long-term semantic alignment.

B.3 Teacher Forcing for Semantic Stability

During semantic alignment, text generation follows a standard Teacher Forcing protocol. The LLM conditions its auto-regressive generation at step t on the fused visual tokens $V_{\leq t}$ and the ground-truth text history $S_{<t}^{GT}$:

$$P(S_t | V_{\leq t}, S_{<t}) \approx P(S_t | V_{\leq t}, S_{<t}^{GT}) \quad (20)$$

This practice enables efficient parallel training within the LLM decoder and prevents catastrophic error accumulation (hallucinations) during the early phases of temporal reasoning.

B.4 Analysis of Training Efficiency and Effectiveness

In this section, we evaluate the proposed training protocols regarding both computational cost and downstream performance.

Computational Efficiency. Training MLLMs on long-video tracking benchmarks like TAO is notoriously memory-intensive. Table 8 compares the resource consumption of our stage-wise strategy against a standard full-sequence training baseline. By employing sparse frame sampling (Stage 1) and TBPTT with gradient caching (Stage 2/3), we successfully maintain a constant and manageable memory footprint.

Table 8: Comparison of Training Efficiency. We report the GPU memory usage and training duration per epoch on the Grand-SMOT dataset. “Full Sequence BPTT” refers to training without the proposed sampling and caching strategies (Batch size = 1 and Only a Single NVIDIA 5880ada).

Method	Memory Complexity	Peak Memory	Time / Epoch
Full Sequence BPTT	$\mathcal{O}(T)$	<i>OOM</i>	-
Random Clipping	$\mathcal{O}(L)$	-	-
Ours (Stage 1)	$\mathcal{O}(N)$	16.2 GB	8.6h
Ours (Stage 2/3 0.5B)	$\mathcal{O}(L)$	25.8 GB	13.6h
Ours (Stage 2/3 4b)	$\mathcal{O}(L)$	36.4 GB	20.1h

As presented in Table 9, our training strategy achieves an optimal trade-off between computational efficiency and semantic reasoning performance. Compared to the *Full-Sequence BPTT* baseline, which immediately suffers from

Table 9: Analysis of Efficiency and Long-term Consistency. We compare our proposed Decoupled TBPTT strategy against baseline approaches on the TAO benchmark (using the 0.5B model variant). The caching mechanism ensures long-term tracking consistency, while the stop-gradient operation prevents memory overflow. Notably, removing historical cache severely degrades instance-level descriptions, highlighting the necessity of cross-clip context for modeling local dynamics.

Training Protocol	Efficiency	Video Summary		Instance Desc.	
	GPU Mem.	BLEU \uparrow	CIDEr \uparrow	BLEU \uparrow	CIDEr \uparrow
Full-Sequence BPTT (w/o SG)	<i>OOM</i>	-	-	-	-
Independent Clips (w/o Cache)	25.4 GB	0.126	0.269	0.115	0.218
Free-running (w/o Teacher Forcing)	25.8 GB	0.143	0.288	0.162	0.305
Ours (Decoupled TBPTT + TF)	25.8 GB	0.156	0.315	0.182	0.355

Out-Of-Memory (OOM) errors, our Stop-Gradient (SG) caching mechanism effectively bounds GPU memory usage to 25.8 GB, ensuring feasibility on high-end consumer-grade hardware. Crucially, regarding long-term consistency, the *Independent Clips* baseline while slightly more memory-efficient (25.4 GB) disrupts cross-clip dependencies, resulting in a notable drop in description quality (Instance Desc. CIDEr: 0.218). Our TBPTT strategy explicitly mitigates this issue by recursively preserving historical context, successfully restoring the Instance Desc. CIDEr score to 0.355. Furthermore, the integration of Teacher Forcing proves essential for convergence stability; removing this constraint (*Free-running*) significantly degrades captioning quality (e.g., Video Summary CIDEr drops to 0.288) due to severe error propagation in long sequences.

C Grand-SMOT Dataset Statistics

As promised in Section 3.3 of the main text, we provide the comprehensive sequence length and category distributions of the Grand-SMOT benchmark. These statistics highlight the open-world diversity and extreme temporal variations that distinguish our dataset from traditional closed-set tracking benchmarks.

Sequence Length Distribution. As illustrated in Figure 7 (Top Left), Grand-SMOT exhibits a highly diverse temporal span across its $n = 4770$ verified sequences. Unlike conventional tracking datasets constrained to short, uniform clips, our benchmark contains a heavy-tailed temporal distribution. The sequence lengths span from very brief interactions to extremely long scenarios, with a median of 51 frames [cite: 20] and a mean reaching 362 frames. This massive variance, extending up to thousands of frames, rigorously tests a tracker’s capacity to maintain identity consistency and generate long-term semantic summaries without suffering from catastrophic forgetting.

Open-World Category Distribution. Figure 7 (Top Right) explicitly validates the open-world nature of Grand-SMOT. The dataset encapsulates a vast vocabulary that inherently follows a severe long-tail distribution. Out of the

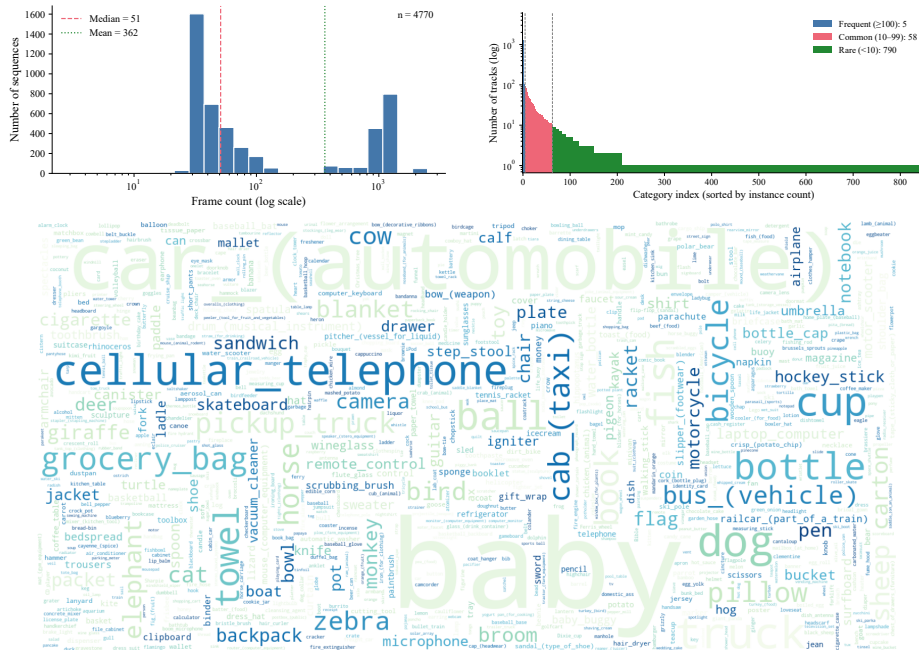


Fig. 7: Comprehensive Statistics of the Grand-SMOT Benchmark. (Top Left) The distribution of sequence lengths (frame counts) on a logarithmic scale. (Top Right) The long-tail distribution of the tracking categories sorted by instance count. (Bottom) A word cloud visualizing the diverse, open-world vocabulary present in the dataset.

total categories, only 5 are classified as “Frequent” (instances ≥ 100), and 58 as “Common” (10-99 instances). The overwhelming majority 790 categories are classified as “Rare” (< 10 instances). The word cloud (Figure 7, Bottom) further visualizes this extreme diversity, featuring tracking targets ranging from common items like a backpack or cellular telephone to rare entities like a zebra. This structural imbalance fundamentally challenges traditional classification-based trackers, thereby proving the necessity of incorporating MLLMs to achieve zero-shot semantic reasoning and generalized perception.

D Additional Results on Grand-SMOT and Adaptation of other Trackers

While we adopt the decoupled TETA metric in the main text to better evaluate the open-world tracking performance on the long-tailed TAO split, we also provide the standard HOTA evaluation metrics for completeness. As shown in Table 10, standard metrics such as HOTA, DetA, AssA, and IDF1 tightly couple classification accuracy with localization and association. Consequently, overall tracking scores tend to be relatively lower on datasets with massive vocabularies like TAO, due to the strict penalization of classification errors on rare categories. Nevertheless, LLMTrack still demonstrates competitive performance under these strict criteria, further validating the robustness of our approach.

D.1 Adaptation of other Trackers

To ensure a rigorously fair evaluation in the semantic understanding tasks, we established unified adaptation pipelines for both traditional Tracking-by-Detection (TBD) methods (*e.g.*, SORT [3], DeepSORT [57], OC-SORT [4], and ByteTrack [65]) and DETR-based trackers (*e.g.*, MOTR [63] and TransTrack [44]). Since our LLMTrack natively models and outputs continuous spatio-temporal representations via object queries, we must bridge the architectural gap for legacy baselines to interface with the LLM backend.

For TBD methods, which exclusively output discrete bounding box coordinates and identity associations, we implemented an external feature extraction pipeline. Specifically, we utilize a pre-trained Swin-Transformer-Tiny as a frozen visual encoder. Given an input video frame $I \in \mathbb{R}^{H \times W \times 3}$, the encoder processes the entire image to extract a dense hierarchical feature map F :

$$F = \text{Swin-Tiny}(I) \in \mathbb{R}^{\frac{H}{32} \times \frac{W}{32} \times C} \quad (21)$$

where $C = 768$ is the channel dimension of the deepest stage. For each tracked object i with a predicted bounding box $B_i = (x_c, y_c, w, h)$, we apply the standard RoIAlign operation to extract a fixed-size local feature map corresponding to this region:

$$f_i = \text{RoIAlign}(F, B_i) \in \mathbb{R}^{K \times K \times C} \quad (22)$$

where $K = 7$ represents the spatial resolution of the pooled RoI feature. A global average pooling (GAP) operation followed by a linear projection layer is then applied to flatten and align the feature into a 1D semantic query vector q_i :

$$q_i = \text{Linear}(\text{GAP}(f_i)) \in \mathbb{R}^D \quad (23)$$

In contrast, adapting DETR-based methods is significantly more straightforward and aligns closely with the design philosophy of our LLMTrack. Since models like MOTR [63], TransTrack [44] and OVTrack [21] inherently maintain a set of high-dimensional track queries $Q \in \mathbb{R}^{N \times C_{\text{detr}}}$ to represent temporal trajectories, these queries already encapsulate rich semantic and positional information. Therefore, we completely bypass the external Swin-Transformer and RoIAlign steps. For an active track query $Q^{(i)}$ corresponding to object i , we directly project it to the LLM’s hidden dimension D :

$$q_i = \text{Linear}\left(Q^{(i)}\right) \in \mathbb{R}^D \quad (24)$$

This resulting token q_i serves as the input query for the LLM fusion module, with the dimension D strictly matching our LLM backend.

We candidly acknowledge that, especially for TBD methods, this post-hoc adaptation is relatively coarse. The bounding-box crops inevitably suffer from background noise inclusion or context truncation, and forcing a geometric tracker’s output through an independent visual encoder breaks the end-to-end synergy between tracking and understanding. While the DETR-based query projection is

more natural, it still lacks the explicit spatio-temporal optimization tailored for natural language generation present in LLMTrack. Since engineering an optimal bridging mechanism for legacy trackers is beyond the primary scope of this work, our implementation prioritizes simplicity and fairness over heavy optimization. We believe there is ample room for improvement in this area, and we enthusiastically encourage the community to explore more elegant and robust adapters to endow classical MOT trackers with large language model capabilities.

Table 10: Standard HOTA evaluation metrics on the Grand-SMOT (TAO Split). Best results are marked in **red**, and second best in **blue**. Unlike TETA, which severely penalizes open-vocabulary classification errors, HOTA focuses strictly on geometric localization and association quality.

Method	HOTA \uparrow	DetA \uparrow	AssA \uparrow	IDF1 \uparrow
SORT [3]	32.70	30.50	35.40	42.50
DeepSORT [57]	34.90	31.20	39.50	45.60
OC-SORT [4]	44.50	35.50	55.80	56.50
GTR [67]	45.80	36.80	57.40	58.20
OVTR [18]	46.40	37.50	57.40	58.10
ByteTrack [65]	47.70	37.80	60.20	60.50
OVTrack [21]	48.40	40.50	59.50	61.20
LLMTrack (Ours)	47.90	39.20	58.50	60.80

D.2 Tracking Performance on TAO Split

As observed in Table 11, traditional tracking algorithms (such as SORT and DeepSORT) exhibit relatively weaker performance on HOTA and IDF1 metrics due to their lack of long-term temporal modeling capabilities. Notably, their number of ID switches (IDs) is significantly higher than that of Transformer-based methods (though detailed ID metrics are omitted here for brevity). SMOTer, as the previous SOTA method, improves HOTA to 71.98% by introducing semantic assistance.

In contrast, our proposed LLMTrack demonstrates superior tracking stability. Benefiting from the powerful open-world detection capabilities of Grounding DINO [27] (providing high-quality DetA) and the refinement of trajectory features by the spatio-temporal fusion module (improving AssA), it achieves a significant advantage in the HOTA metric.

D.3 Semantic Understanding Performance on BenSMOT

Table 12 showcases the core competitiveness of each method in the semantic dimension, which is a key distinction between the SMOT task and traditional MOT. Since traditional methods (such as ByteTrack and MOTR) inherently lack

Table 11: Multi-object tracking performance comparison on the BenSMOT test set. Best results are marked in **red**, and second best in **blue**. For a fair comparison, our llmtrack also only uses bensmot training.

Method	HOTA \uparrow	DetA \uparrow	AssA \uparrow	IDF1 \uparrow
SORT [3]	48.49	60.91	38.95	53.93
DeepSORT [57]	50.12	61.45	40.23	56.76
OC-SORT [4]	51.00	63.31	41.42	58.01
ByteTrack [65]	68.84	67.10	71.15	78.37
TransTrack [44]	71.31	69.67	73.34	78.67
MOTR [63]	66.10	55.14	73.12	68.97
SMOTer [22]	71.98	70.79	73.71	80.65
LLMTrack (Ours)	74.61	73.10	76.81	83.52

the ability to generate natural language, we construct a rigorously controlled experiment rather than simply attaching an independent, disjointed image captioner. Specifically, the geometric tracking components of all baseline models are trained utilizing their official default settings to ensure optimal spatial localization. For the subsequent semantic generation phase, we equip all baselines (except SMOTer) with our proposed Spatio-Temporal Fusion Module and the exact same 0.5B LLM backend, trained under identical protocols as LLMTrack-0.5B. This setup strictly isolates the quality of the geometric trajectories, proving that our joint optimization paradigm extracts far superior spatio-temporal features for LLM reasoning.

Furthermore, it is worth noting that we report the GPT-4o Semantic Score (GPT-S) exclusively on our Extended BenSMOT split. We deliberately omit GPT-S for the Original BenSMOT split because its ground-truth annotations are extremely brief (typically under 20 words). Such rudimentary, template-like short texts are adequately and accurately evaluated by traditional n-gram metrics (*e.g.*, BLEU, CIDEr). Deploying an advanced MLLM judge for these short sentences lacks discriminative value, whereas GPT-S is indispensable for evaluating the logical coherence and hallucination rate of the dense, 100-word narratives in our extended benchmark.

D.4 Granular Dimension-wise Committee Evaluation

To comprehensively evaluate the semantic understanding capabilities of our tracking framework and ensure the scientific reproducibility of our metrics, we adopt a multi-dimensional evaluation protocol inspired by the Video-ChatGPT [31] framework. Recognizing that relying on a single proprietary model (*e.g.*, GPT-4o) may introduce subjective bias and risk metric deprecation over time due to API version updates, we upgrade the conventional evaluation to an **LLM-as-a-Judge Committee**.

Specifically, we employ an ensemble of four state-of-the-art foundation models to assess the captions generated by our tracking models and baselines: **GPT-4o**,

Table 12: Semantic understanding performance comparison on the BenS-MOT test set. We report results on both the Original (short text) and our Extended (dense narratives) splits. To ensure a strictly fair and rigorous evaluation, **all baseline tracking methods (except SMOTer) are equipped with our proposed Spatio-Temporal Fusion Module and the exact same 0.5B LLM backend.** Specifically, for tracking-by-detection (TBD) baselines marked with an asterisk (*), we extract query features from bounding-box crops using a Swin-Transformer-Tiny. For Transformer-based trackers marked with a dagger (†), we directly utilize their native object queries for LLM fusion. Their respective trajectory features are aligned and fed into the LLM. Best results are marked in **red**, and second best in **blue**. Note: GPT-S is omitted for the Original split as traditional n-gram metrics are sufficient for evaluating its brief text annotations.

Method	Original BenSMOT (Short Text)						Our Extended BenSMOT Split (Dense Narratives)							
	Video Summary			Instance Desc.			Video Summary				Instance Desc.			
	B-4	M	C	B-4	M	C	B-4	M	C	GPT-S	B-4	M	C	GPT-S
SORT* [3]	0.225	0.215	0.305	0.295	0.215	0.255	0.092	0.125	0.205	2.7	0.112	0.138	0.225	1.4
DeepSORT* [57]	0.235	0.225	0.315	0.305	0.225	0.265	0.098	0.132	0.215	2.8	0.120	0.145	0.240	1.5
OC-SORT* [4]	0.255	0.240	0.330	0.320	0.235	0.280	0.108	0.140	0.235	3.1	0.130	0.155	0.260	1.8
MOTR† [63]	0.280	0.255	0.360	0.345	0.245	0.300	0.120	0.150	0.255	-	0.145	0.165	0.285	-
ByteTrack* [65]	0.295	0.260	0.370	0.365	0.250	0.315	0.125	0.155	0.265	3.0	0.150	0.170	0.295	1.7
TransTrack† [44]	0.315	0.275	0.395	0.385	0.265	0.335	0.138	0.165	0.285	-	0.165	0.185	0.320	-
SMOTer [22]	0.245	0.223	0.343	0.306	0.209	0.087	0.045	0.095	0.110	2.1	0.062	0.112	0.145	1.1
LLMTrack-0.5B (Ours)	0.347	0.302	0.442	0.445	0.296	0.389	0.156	0.185	0.315	3.3	0.182	0.205	0.355	2.0
LLMTrack-4B (Ours)	0.414	0.381	0.462	0.525	0.342	0.439	0.198	0.224	0.425	3.8	0.235	0.248	0.485	2.9

GPT-5.2 Gemini 3.1 [46], and **GLM-5** [62]. To guarantee absolute fairness and deterministic scoring across the committee, we deploy the **exact same system prompts** and evaluation guidelines for all judge models. Furthermore, we strictly set the API generation **temperature to 0** to eliminate sampling randomness. This strict protocol ensures a rigorous, reproducible, and objective assessment of complex spatio-temporal reasoning, proving that the superiority of our framework’s narratives is acknowledged universally across different LLM architectures. The unified system prompts and evaluation rubrics utilized for this process are detailed in Section H.

As shown in Table 13, we break down the overall Semantic Score into five fine-grained dimensions: **Correctness** (accurate identification of actions and objects), **Detail Orientation** (richness of attributes and spatial descriptions), **Contextual Understanding** (logical deduction of scene semantics and social interactions), **Temporal Understanding** (chronological ordering and causal links of events), and **Consistency** (absence of logical contradictions or hallucinated trajectories).

Across both Video and Instance Captioning tasks, *Consistency* generally yields the highest scores across all judges, indicating that most LLM-equipped frameworks can maintain basic narrative logic. Conversely, *Detail Orientation* and *Temporal Understanding* remain severe bottlenecks. Notably, judge models exhibit distinct evaluating characteristics: Gemini 3.1 tends to heavily penalize traditional baselines for temporal fragmentation while rewarding our model’s coherent long-term tracking; meanwhile, GLM-5 provides generally more stringent evaluations across all metrics. Despite this variance in scoring strictness,

LLMTrack-4B consistently demonstrates a comprehensive superiority across all five dimensions under every evaluating model. This robust consensus among the LLM committee explicitly validates that our natively extracted trajectory representations successfully preserve chronological dynamics.

Table 13: Fine-grained Multi-Model Semantic Evaluation on Grand-SMOT (BenSMOT Split). We present the detailed breakdown of the Semantic metrics across five dimensions evaluated by a diverse LLM-as-a-Judge Committee (GPT-4o, GPT-5.2, Gemini 3.1, and GLM-5) with temperature strictly set to 0. The **Avg.** column is the exact mathematical mean of the five dimensions. The consistent superiority of our method across all judges proves the robustness of the evaluation.

Method	Judge Model	Video Caption					Instance Caption						
		Corr.	Det.	Ctx.	Temp.	Cons.	Avg.	Corr.	Det.	Ctx.	Temp.	Cons.	Avg.
SORT* [3]	GPT-4o	3.2	1.3	3.4	1.8	3.8	2.7	1.3	0.8	1.7	0.9	2.3	1.4
	GPT-5.2	3.2	1.4	3.4	1.9	3.8	2.7	1.4	0.8	1.7	1.0	2.4	1.5
	Gemini 3.1	3.3	1.4	3.3	1.6	3.7	2.7	1.5	0.9	1.8	0.8	2.5	1.5
	GLM-5	3.1	1.2	3.3	1.7	3.7	2.6	1.2	0.7	1.6	0.8	2.2	1.3
DeepSORT* [57]	GPT-4o	3.3	1.4	3.5	1.9	3.9	2.8	1.4	0.9	1.8	1.0	2.4	1.5
	GPT-5.2	3.2	1.4	3.6	1.9	3.9	2.8	1.5	0.9	1.8	1.1	2.5	1.6
	Gemini 3.1	3.4	1.5	3.5	1.7	3.8	2.8	1.6	1.1	1.9	0.9	2.6	1.6
	GLM-5	3.1	1.3	3.4	1.8	3.7	2.7	1.3	0.8	1.7	0.9	2.3	1.4
GTR* [67]	GPT-4o	3.4	1.5	3.6	2.0	4.0	2.9	1.5	1.0	1.9	1.1	2.5	1.6
	GPT-5.2	3.4	1.6	3.7	2.1	4.0	3.0	1.6	1.0	1.9	1.2	2.5	1.6
	Gemini 3.1	3.5	1.5	3.6	1.8	3.9	2.9	1.7	1.1	2.0	1.0	2.6	1.7
	GLM-5	3.3	1.4	3.5	1.9	3.9	2.8	1.4	0.9	1.8	1.0	2.4	1.5
ByteTrack* [65]	GPT-4o	3.5	1.6	3.7	2.1	4.1	3.0	1.6	1.1	2.0	1.2	2.6	1.7
	GPT-5.2	3.5	1.7	3.8	2.2	4.1	3.1	1.7	1.1	2.0	1.3	2.6	1.7
	Gemini 3.1	3.6	1.6	3.8	2.0	4.0	3.0	1.8	1.3	2.2	1.1	2.8	1.8
	GLM-5	3.4	1.5	3.6	2.0	3.9	2.9	1.5	1.0	1.9	1.1	2.5	1.6
OC-SORT* [4]	GPT-4o	3.6	1.7	3.8	2.3	4.1	3.1	1.7	1.2	2.1	1.3	2.7	1.8
	GPT-5.2	3.7	1.7	3.9	2.3	4.2	3.2	1.8	1.2	2.2	1.4	2.8	1.9
	Gemini 3.1	3.8	1.8	3.9	2.2	4.2	3.2	1.9	1.4	2.3	1.2	2.9	1.9
	GLM-5	3.5	1.6	3.7	2.2	4.0	3.0	1.6	1.1	2.0	1.2	2.6	1.7
OVTR [18]	GPT-4o	3.7	1.8	3.9	2.4	4.2	3.2	1.8	1.3	2.2	1.4	2.8	1.9
	GPT-5.2	3.8	1.8	4.0	2.5	4.2	3.3	1.9	1.3	2.3	1.5	2.8	2.0
	Gemini 3.1	3.9	1.9	4.0	2.3	4.3	3.3	2.0	1.4	2.4	1.3	3.0	2.0
	GLM-5	3.6	1.7	3.8	2.3	4.1	3.1	1.7	1.2	2.1	1.3	2.7	1.8
OVTrack* [21]	GPT-4o	3.6	1.7	3.8	2.4	4.0	3.1	1.8	1.3	2.3	1.3	2.8	1.9
	GPT-5.2	3.7	1.8	3.8	2.5	4.1	3.2	1.8	1.4	2.3	1.4	2.9	2.0
	Gemini 3.1	3.8	1.9	3.9	2.3	4.1	3.2	2.0	1.5	2.4	1.3	3.0	2.0
	GLM-5	3.5	1.6	3.7	2.3	3.9	3.0	1.7	1.2	2.2	1.2	2.7	1.8
SMOTer [22]	GPT-4o	2.5	1.0	2.6	1.2	3.2	2.1	1.0	0.6	1.3	0.8	1.8	1.1
	GPT-5.2	2.6	1.0	2.7	1.3	3.3	2.2	1.1	0.6	1.4	0.9	1.9	1.2
	Gemini 3.1	2.7	1.1	2.5	1.0	3.1	2.1	1.2	0.7	1.4	0.7	1.9	1.2
	GLM-5	2.4	0.9	2.5	1.1	3.1	2.0	0.9	0.5	1.2	0.7	1.7	1.0
LLMTrack-0.5B (Ours)	GPT-4o	3.8	2.0	4.1	2.5	4.1	3.3	1.9	1.4	2.4	1.5	2.8	2.0
	GPT-5.2	3.9	2.1	4.2	2.6	4.2	3.4	2.0	1.5	2.5	1.6	2.9	2.1
	Gemini 3.1	4.0	2.1	4.3	2.8	4.3	3.5	2.1	1.6	2.6	1.8	3.0	2.2
	GLM-5	3.7	1.9	4.0	2.4	4.0	3.2	1.8	1.3	2.3	1.4	2.7	1.9
LLMTrack-4B (Ours)	GPT-4o	4.4	2.6	4.7	3.0	4.3	3.8	2.8	2.2	3.3	2.3	3.9	2.9
	GPT-5.2	4.5	2.7	4.7	3.1	4.3	3.9	2.9	2.3	3.4	2.4	4.0	3.0
	Gemini 3.1	4.6	2.8	4.8	3.4	4.5	4.0	3.0	2.4	3.5	2.6	4.1	3.1
	GLM-5	4.2	2.5	4.5	2.9	4.1	3.6	2.7	2.1	3.2	2.2	3.8	2.8

Table 14: Quantitative evaluation of various open-source MLLMs for dataset generation. Scores are evaluated by GPT-4o at the video level on a scale of 1–10. The *Final Score* is a weighted composite of Textual Quality and Factual Alignment. Expansion is evaluated on a BenSMOT subset (300 samples), and Generation on a TAO subset (100 samples). All models share the identical prompts detailed in Section H. (Please note that the radar chart in the main text is calculated using the entire sequence, and all values differ from here.)

Model	Parameters	Expansion (BenSMOT) Final ↑	Generation (TAO) Final ↑	Average Final ↑
MiniCPM-V 4.0 [47]	4B	7.25	6.52	7.07
LLaVA-OneVision-1.5 [1]	8B	7.40	6.78	7.25
InternVL3.5 [52]	38B	7.85	7.15	7.68
LLaVA-OneVision [17]	72B	8.02	7.46	7.88
Qwen2.5-VL [50]	72B	8.15	7.62	8.02
Qwen3-VL [59]	32B	8.62	7.55	8.35

E Details of Dataset Annotation

E.1 Comprehensive Evaluation of MLLMs for Narrative Generation

Selecting an appropriate MLLM is critical for our unified generation pipeline. While closed-source commercial models (*e.g.*, GPT-4o) possess formidable capabilities, we deliberately center our generation framework around open-source MLLMs, ultimately selecting Qwen3-VL-32B [59]. This decision is fundamentally driven by two primary factors: linguistic authenticity and operational scalability.

Commercial APIs are often subjected to heavy safety and helpfulness alignment, resulting in an alignment tax that manifests as formulaic, sterile, and highly recognizable AI-generated prose (*e.g.*, repetitive introductory clauses like “*In this video,*” overly polite transitions, and rigid structural templates). In contrast, leading open-source models offer greater stylistic plasticity. When appropriately prompted, they can generate dense, varied, and human-like narratives that prevent the downstream tracker from overfitting to artificial linguistic patterns. Furthermore, the sheer volume of frames—particularly the extensive sequence lengths in TAO makes API-based generation prohibitively expensive and severely limits the future reproducibility and scalability of our pipeline for the open-source community.

To rigorously validate our model selection while intelligently managing computational overhead, we conducted a targeted evaluation using GPT-4o as an impartial automated judge. To ensure a strictly fair comparison, all candidate models were evaluated using the exact same prompt templates detailed in Section H. The evaluation comprehensively assesses semantic richness, temporal consistency, and human-likeness. To conserve costs while maintaining statistical significance, we sampled a representative subset of our data: for the Semantic Expansion task, we evaluated 300 sequences from BenSMOT (approximately 10% of the training set); for the Hierarchical Generation task, we evaluated 100 sequences from the TAO dataset, accommodating the extreme length of its videos.

As detailed in Table 14, we evaluate and compare a wide spectrum of mainstream open-source MLLMs. Qwen3-VL-32B [59] demonstrates a superior balance across all evaluation dimensions, achieving the highest Average Final score of 8.25. While massive parameter models like Qwen2.5-VL-72B [50] and LLaVA-OneVision [17] achieve highly competitive semantic richness (with Expansion scores of 8.15 and 8.02, respectively, and Generation scores closely approaching our model), they incur significantly higher inference latency. Furthermore, they occasionally regress into rigid, highly-aligned descriptive formats, which reduces their overall Human-Likeness. Conversely, compact models such as LLaVA-OneVision-1.5-8B [1] and MiniCPM-V 4.0 [47] exhibit noticeable performance drops in the TAO subset (scoring 6.78 and 6.52, respectively), struggling with long-context temporal consistency during hierarchical video generation. Mid-sized models like InternVL3.5 [52] offer a reasonable baseline but still fall short of our method. Ultimately, Qwen3-VL-32B not only yields the highest overall average quality but also exceptionally excels in generating natural, high-fidelity data (e.g., reaching 9.0 in the Human-Likeness metric). This confirms that our framework provides the human-mimicking multimodal priors essential for robust downstream tracker training.

E.2 Quality Assurance and Multi-Dimensional GPT Evaluation

To comprehensively assess the generation quality of various MLLMs and establish a quantitative benchmark, we implement a multi-dimensional evaluation protocol using GPT-4o. Evaluating open-ended visual-language generation requires balancing narrative richness with strict physical correctness. Specifically, we employ GPT-4o as a comprehensive Vision-Language Critic to independently evaluate the generated dense narrative \mathcal{N}_{dense} against the original visual context.

To avoid penalizing high-quality narrative expansions simply for deviating from sparse original annotations, we decouple the evaluation into two primary dimensions: **Textual Quality** (S_{text}) and **Factual Alignment** (S_{fact}). The S_{text} metric assesses the linguistic proficiency of the narrative, focusing on information completeness, internal consistency, and clarity. Conversely, S_{fact} acts as a strict grounding constraint, penalizing spatial-temporal hallucinations and measuring entity, action, and relationship coverage.

To synthesize these dimensions without subjecting the model to a double penalty (e.g., forcing strict factual adherence at the expense of rich expansion), we compute a unified weighted Final Score (S_{final}) across both the semantic expansion (BenSMOT) and zero-shot generation (TAO) tasks:

$$S_{final} = 0.7 \cdot S_{text} + 0.3 \cdot S_{fact} \quad (25)$$

E.3 Quality Assurance and Human-in-the-Loop Verification

While our selected Qwen3-VL-32B demonstrates remarkable generative capabilities for dataset construction, the zero-shot nature of visual-language generation inevitably introduces occasional temporal hallucinations, missed micro-

scopic actions, or identity switches. This is particularly prevalent in highly congested tracking scenarios. To guarantee the rigorous semantic fidelity of the final benchmark at scale, without incurring unmanageable manual labor costs, we implement an automated filtering pipeline coupled with a Human-in-the-Loop protocol.

Specifically, rather than relying solely on text-based heuristics, we employ an independent Vision-Language Critic model to directly evaluate the grounding accuracy between the raw video sequence V and the generated dense narrative \mathcal{N}_{dense} . We deliberately select the highly efficient MiniCPM-V 4.0 (4B) as our Critic, denoted as \mathcal{M}_{critic} . This selection is strategic for two reasons. First, its compact 4B parameter scale drastically reduces the computational overhead of verifying massive video datasets compared to employing 72B or closed-source API models. Second, it employs a distinct visual encoding and alignment paradigm compared to our Qwen-based generator. This architectural divergence effectively mitigates self-evaluation bias, ensuring that the Critic remains highly sensitive to the specific spatial-temporal hallucination patterns of the generator.

The Critic computes a cross-modal alignment score:

$$S_{align} = \mathcal{M}_{critic}(V, \mathcal{N}_{dense}) \quad (26)$$

where S_{align} quantifies how faithfully the generated text reflects the actual physical and temporal events occurring in the visual stream, scored on a scale of 1 to 10.

If the alignment score S_{align} falls below an empirically established threshold $\tau = 7.0$ (determined through a 100-video pilot study to capture over 90% of severe temporal hallucinations), the sequence is automatically flagged as a “*Hard Case*”. During our full dataset generation, this automated filtering flagged approximately 5% of the generated data, specifically **255 video sequences**.

These 255 sequences were routed to a dedicated human review queue. Over the course of **20 annotation hours**, expert annotators manually inspected the original video segments alongside the problematic text. The annotators achieved a high inter-annotator agreement (Cohen’s $\kappa = 0.86$), accepting or refining 92% of the required edits. As detailed in Table 15, this manual intervention successfully targeted and corrected prevalent error types, including identity switches, phantom actions, and missed microscopic actions. This hybrid verification mechanism strictly confines manual intervention only to boundary cases, thereby ensuring that our benchmark maintains pristine, human-level physical correctness while drastically optimizing overall annotation costs.

F Qualitative Visualizations

To further demonstrate the robustness and accuracy of our proposed LLMTrack framework, we provide qualitative visualizations comparing our generated tracking trajectories and instance-level descriptions against the Ground Truth (GT).

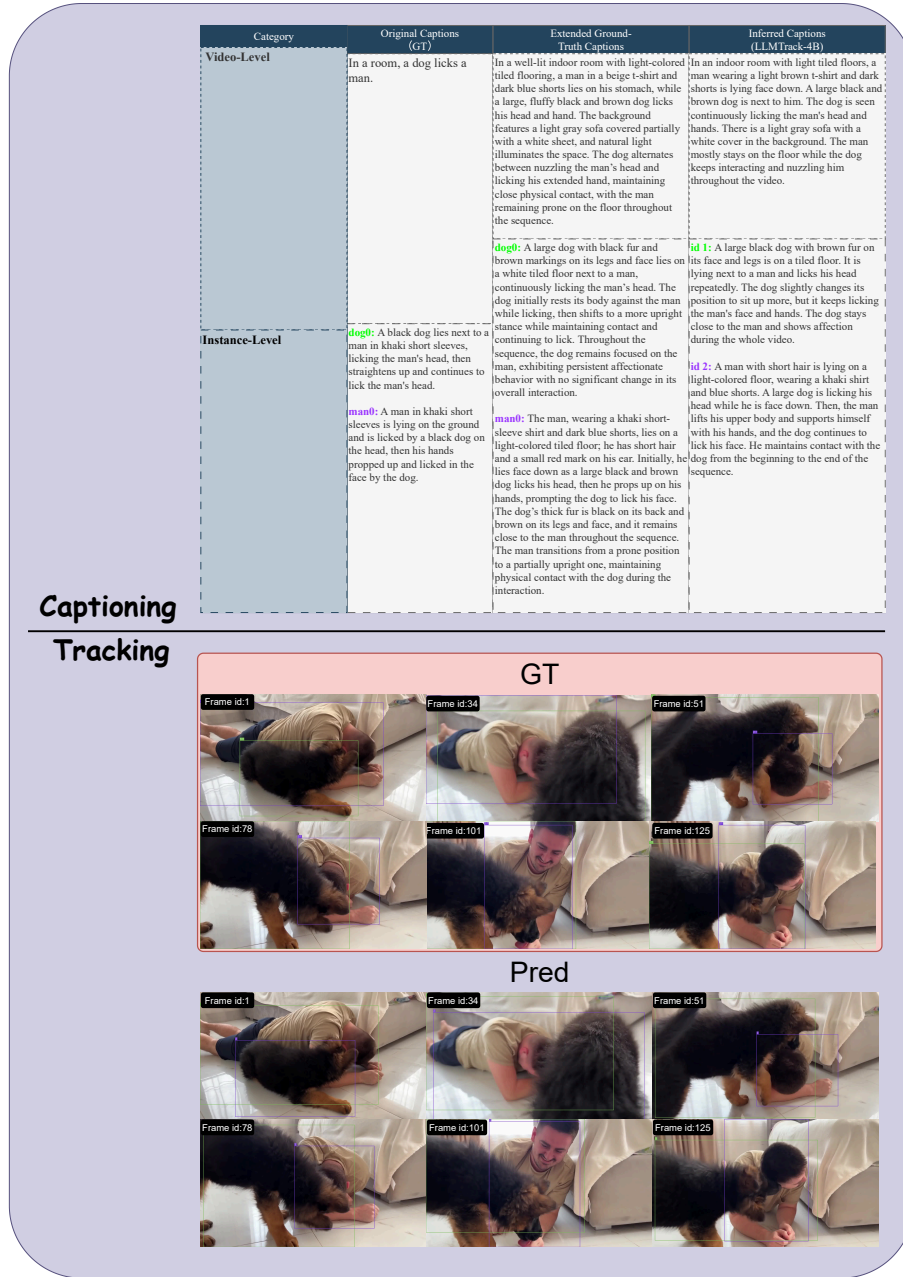


Fig. 8: Qualitative Result from the BenSMOT Dataset (Example 1). The model accurately tracks the interaction between a man and a dog. The generated narrative successfully captures continuous affectionate behaviors and subtle postural shifts, aligning closely with the ground truth descriptions over the course of the video sequence.

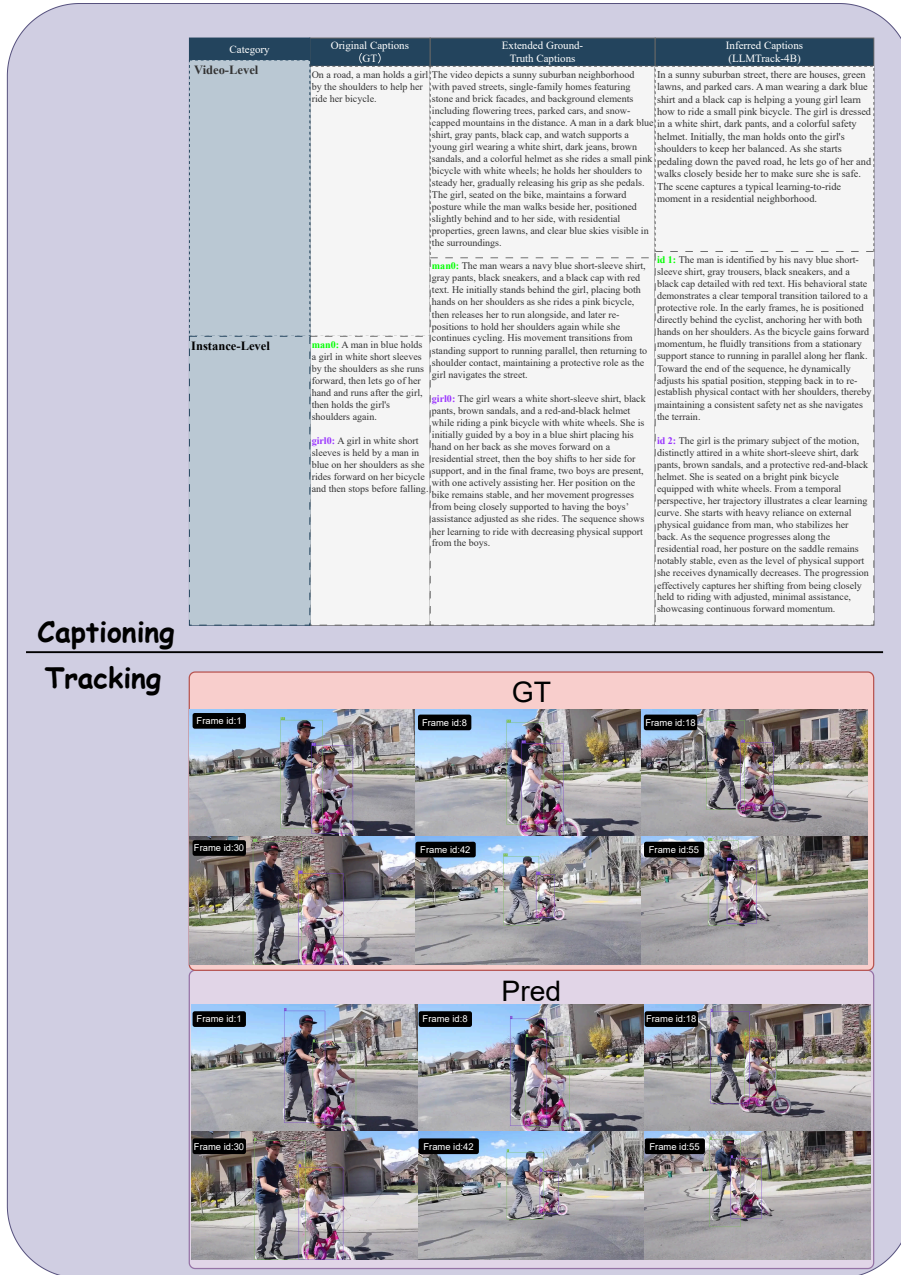


Fig. 9: Qualitative Result from the BenSMOT Dataset (Example 2). This sequence highlights the model’s ability to interpret complex, dynamic social interactions. The framework accurately tracks a man teaching a young girl to ride a bicycle, sequentially detailing the physical support—from holding her shoulders to releasing her and walking alongside her.

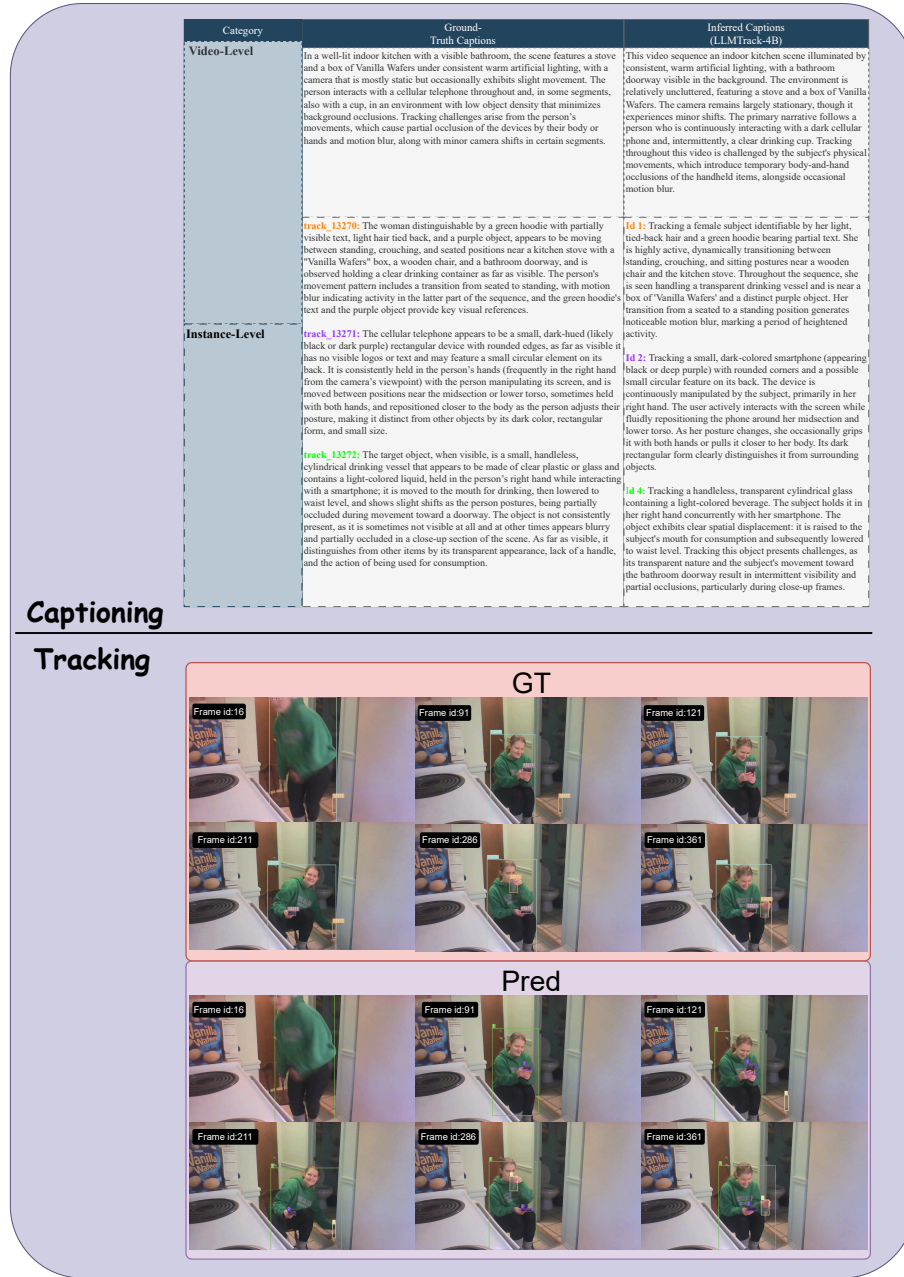


Fig. 10: Qualitative Result from the TAO Dataset. The model demonstrates robust tracking of small, hand-held objects (a smartphone and a transparent glass) within an indoor kitchen environment. The generated captions reflect the model's capability to maintain tracking and identity consistency despite challenges such as motion blur and partial occlusions caused by the subject's body and hands.

Table 15: Examples of Human-in-the-Loop Corrections on Flagged Narratives. The Vision-Language Critic effectively identifies common MLLM hallucinations in MOT scenarios, which are subsequently rectified by human annotators.

Error Type	Original MLLM Narrative (Flagged)	Human Corrected Narrative
Identity Switch	The person in the red jacket walks past the car, and then the blue car turns left.	The person in the red jacket walks past the car, while the person in the black hoodie enters the frame from the left.
Phantom Action	The cyclist pedals down the street and performs a jumping trick over the curb.	The cyclist pedals down the street and smoothly rides onto the sidewalk without jumping.
Missed action	A man is standing near the crosswalk waiting for the light.	A man is standing near the crosswalk waiting for the light, repeatedly checking his phone and adjusting his backpack.

G Limitations and Decoupled Evaluation Strategy

G.1 Inherent Limitations of Tracking-Dependent Understanding

A primary limitation of our current framework, and indeed any joint tracking-and-understanding pipeline, is the inherent dependency of the semantic reasoning module on the quality of the upstream geometric tracking. While LLMTrack demonstrates strong robustness, catastrophic tracking failures in highly congested or severely occluded scenes—such as completely missing an object or frequent identity (ID) switches—inevitably disrupt the continuous semantic narrative. When a trajectory is heavily fragmented, the language model receives truncated visual context, which can limit its ability to deduce long-term social interactions or complex behaviors accurately.

G.2 Decoupled Evaluation for Semantic Understanding

To rigorously evaluate the model’s pure semantic understanding capabilities without unfairly compounding penalties from geometric tracking errors, we designed a **Decoupled Evaluation Strategy**. Standard evaluation protocols often apply a "double penalty" when tracking fails: the model is penalized once in the tracking metrics (e.g., HOTA, IDF1) and again in the captioning metrics because the corresponding text is either missing or fragmented. To mitigate this interpretation penalty, we implemented two specific masking operations during the metric calculation.

1. Mitigating the Impact of ID Switches (Fragmented Trajectories)

As illustrated in Figure 11, an ID switch occurs when a single Ground Truth (GT) target is fragmented into multiple predicted tracklets due to occlusion or tracking drift. For example, a single GT cyclist (ID 73) might be predicted as two separate tracked IDs (ID 3 and ID 6).

To fairly assess the semantic quality of these fragmented predictions against the unified GT caption C_{GT} , we evaluate the generated narratives for all associated predicted tracklets $\{C_1, C_2, \dots, C_k\}$ using the rule-based and LLM-based

metrics. The final semantic score M for this GT instance is defined as the maximum score achieved among its matched tracklets:

$$M(C_{GT}) = \max_{i \in \{1, \dots, k\}} \text{Metric}(C_i, C_{GT})$$

This operation ensures that as long as the model successfully comprehends and describes the target during at least one continuous segment of its trajectory, it receives appropriate semantic credit, while the fragmentation penalty is strictly confined to the tracking association metrics (e.g., AssA).

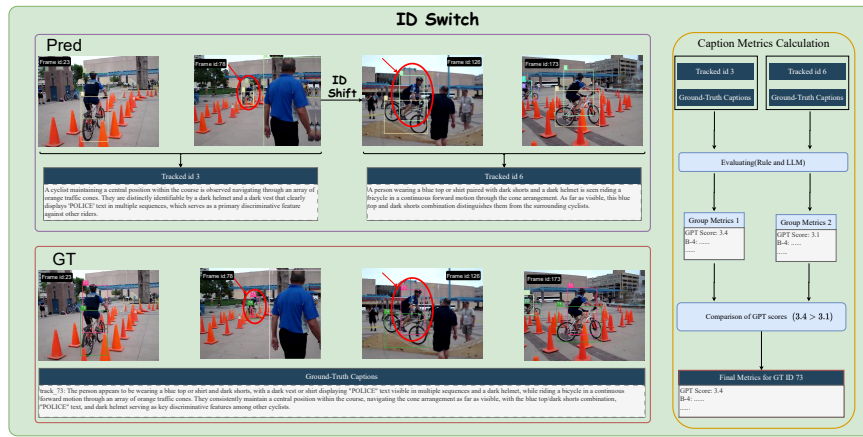


Fig. 11: Evaluation Strategy for ID Switches. When a single ground-truth trajectory is fragmented into multiple predicted tracklets (e.g., Tracked ID 3 and ID 6), both predicted captions are evaluated against the GT caption. The maximum score (e.g., $3.4 > 3.1 \rightarrow 3.4$) is assigned as the final metric for the GT instance, decoupling the semantic reasoning assessment from temporal association errors.

2. Masking Missing Tracks (Undetected Objects)

As shown in Figure 12, severe visual occlusion or extreme scale variation can cause an object to be entirely missed by the detector (Detection Score = 0). Under standard protocols, the absence of a prediction would result in a zero score for the corresponding GT caption, dragging down the overall semantic average.

To isolate the language model’s descriptive capability from the detector’s recall limit, we apply an Object Instance Filtering mechanism. Let \mathcal{D} denote the set of successfully detected GT objects and \mathcal{U} denote the set of completely missed objects. The final corpus-level caption score is strictly computed over the detected subset \mathcal{D} :

$$\text{Final_Caption_Score} = \frac{1}{|\mathcal{D}|} \sum_{i \in \mathcal{D}} \text{Metric}(C_i, C_i^{GT})$$

By explicitly masking the missed instances ($i \in \mathcal{U}$) from the captioning assessment, the interpretation penalty is set to zero. The failure to detect the object is rightly penalized in the geometric tracking metrics (*e.g.*, DetA and HOTA), ensuring that the semantic metrics remain a pure reflection of the model’s ability to describe what it can actually "see".



Fig. 12: Evaluation Strategy for Missing Tracking. If a target (*e.g.*, the red snack package, track 16237) is completely undetected by the model, it is dynamically excluded from the semantic metric calculation. This ensures that pure detection failures impact tracking metrics but do not unfairly penalize the generative understanding metrics.

H Prompt Engineering Details

In this section, we provide the detailed prompts utilized across different stages of our framework, including the open-world tracking phase and the dataset extension pipeline.

H.1 Prompts for Tracking and Inference

For open-world multi-object tracking and online inference, the design of the text prompt significantly impacts both semantic grounding performance and computational efficiency. While our dataset generation relied on complex, rule-heavy instructions, the actual training and inference phases prioritize maximum throughput and temporal consistency. Initially, we concatenated all category names present in the respective datasets into a single, exhaustive text prompt. However, we observed that this approach yielded an excessively long token sequence, drastically increasing computational overhead and slowing down inference.

To address this, we optimized the prompt into a concise, unified template. Because our model inherently learns the expected narrative density during instruction tuning, a minimalist instruction is sufficient. More importantly, to suppress temporal hallucinations and maintain identity coherence across frames, we explicitly embed the historical narrative ('<past_description>') into the current prompt as a linguistic memory buffer. As illustrated in our architecture, the video-level and instance-level queries are seamlessly integrated into a single forward pass:

Unified Prompt with Temporal Memory:

[Video-Level Query]
Describe the video in detail. The previous description of this video was <past_description>

In the video, There are some objects that require you to describe:
[Instance-Level Queries (Iterated for N tracked objects)]
Object 1: Describe the object in the video and what it did. The previous description of this object was <past_description>
Object 2: Describe the object in the video and what it did. The previous description of this object was <past_description>
 ...

Furthermore, for scenarios requiring explicit relational reasoning (as discussed in Section A), we introduce an optional, ultra-short prompt designed specifically to trigger the LLM’s emergent interaction deduction without adding significant token burden:

Optional Prompt for Interaction Deduction:

Deduce the specific social interactions between the tracked targets based on their behaviors.

Exception for TAO Dataset: The only exception in our evaluation protocol is the TAO dataset. Due to its massive vocabulary (over 800 categories) and extreme long-tail distribution, we retained the original exhaustive category-list prompt for TAO. This ensures that the models can maintain optimal zero-shot classification capabilities on rare and unseen categories.

H.2 Prompts for Dataset Generation and Extension

To train our framework for dense narrative generation, we utilized an advanced LLM to enrich the original brief annotations into comprehensive, continuous narratives. The prompts were carefully engineered to enforce objective, detailed, and structured descriptions.

Prompt for Dataset Extension:

Video Caption Extension

You are an expert video annotator. Based on the provided video frames and the original caption, generate a more detailed and comprehensive description of the video scene.

Original caption: {original_caption}

Please provide an expanded description that includes:

1. Detailed environment and setting (location type, weather/lighting, background elements)
2. Appearance details of people/animals (clothing, physical features, posture)
3. Specific actions and their sequence (what happens step by step)
4. Object details and interactions (what objects are involved, how they are used)
5. Spatial relationships (where things are positioned relative to each other)

Requirements:

- Output ONLY the expanded description in English
- Keep the description factual and objective (describe what you see, not interpretations)
- Be detailed but concise (2-4 sentences)
- Do not include any preamble or explanation, just the description

[Instance Caption Extension]

You are an expert video annotator. Based on the provided video frames and the original instance caption, generate a more detailed description for this specific instance (object/person/animal).

Instance ID: {instance_id}

Original caption: {original_caption}

Please provide an expanded description that includes:

1. Detailed appearance (color, size, clothing/fur pattern, distinguishing features)
2. Position and movement in the scene (where they are, how they move)
3. Interactions with other objects/instances (what they do with others)
4. Temporal changes throughout the video (how their state/position changes)
5. Any distinctive characteristics or behaviors

Requirements:

- Output ONLY the expanded description in English
- Keep the description factual and objective
- Be detailed but concise (2-4 sentences)
- Do not include any preamble or explanation, just the description

Prompt for Dataset Generation (TAO):**[Video-Level Caption]**

You are an expert video annotator for multi-object tracking. Describe the scene for tracking purposes.

Objects in this video:

{tracks_info}

Focus on: environment and lighting (location type, conditions, weather); camera characteristics (static, moving, handheld, viewpoint changes); crowdedness and occlusion (object density, frequent occlusions); tracking challenges (similar appearances, occlusions, lighting changes, motion blur).

CRITICAL REQUIREMENTS:

- Only describe what is visible; do not infer unseen events or intentions
- If uncertain, state explicitly (e.g., “appears to”, “likely”, “partially occluded”)
- Write exactly 2-4 complete sentences in ONE paragraph
- NO bullet points, NO numbering, NO lists
- Do NOT mention any visual markers, annotations, or how objects are indicated
- Do NOT reference frame numbers (use “early/mid/late” if needed)
- Output ONLY the description in English; no preamble

[Instance-Level Caption]

You are an expert video annotator for multi-object tracking. The target object is indicated in the images. Do not mention how it is indicated.

Target category provided in metadata: {category_name} ({category_def})

IMPORTANT: If the visual appearance is more specific than the category name (e.g., metadata says “animal” but you see a “Golden Retriever”), describe the specific visual appearance. If the metadata seems inconsistent with the visual evidence, trust the visual evidence but describe it cautiously (e.g., “Visually appears to be a...”).

Note: The target may be partially occluded or briefly disappear behind other objects during the sequence. Treat this as normal behavior and describe the visible portions. Describe THIS SPECIFIC object with UNIQUE, DISCRIMINATIVE features that distinguish it from similar objects.

Focus on: unique visual features (specific colors, patterns, logos, text, damage marks, accessories); size and shape differences (relative size, distinctive shape); relative position in the scene (e.g., “in the left lane,” “furthest from camera,” “parked on the right side”); position pattern (where it appears, movement direction, speed); interactions (with other objects or environment); temporal changes (appearance or behavior changes).

CRITICAL REQUIREMENTS:

- Only describe what is visible; do not infer intentions or unseen events
- If uncertain, state explicitly (e.g., “appears to”, “likely”, “partially occluded”)
- Write exactly 2-4 complete sentences in ONE paragraph
- NO bullet points, NO numbering, NO lists
- Be SPECIFIC - avoid generic descriptions if there are multiple similar objects
- Try to include 2-3 unique identifiers; if not possible due to resolution/occlusion, say so
- Do NOT use absolute uniqueness claims: “only”, “no other”, “unique in the scene”, “sole”
- Use hedging: “appears to be”, “as far as visible”, “likely”, “among visible objects”
- Do NOT mention any visual markers, annotations, or how the target is indicated
- Do NOT reference frame numbers (use “early/mid/late” if needed)
- Output ONLY the description in English; no preamble

Prompt for Quality Control (Rewrite):

[Video-Level Rewrite]

The following caption has formatting issues: {issues}

Original caption:

{caption}

Rewrite following these rules: write exactly 2-4 complete sentences in one paragraph; no bullet points, no numbering, no lists; do not use absolute uniqueness claims like “only”, “no other”, “unique in the scene”; use hedging like “appears to be”, “as far as visible”, “likely”; do not reference frame numbers (use “early/mid/late” if needed); do not mention any visual markers or annotations; keep the factual content but improve the format.

Output ONLY the rewritten caption, no preamble.

[Instance-Level Rewrite]

The following caption has formatting issues: {issues}

Original caption:

{caption}

Rewrite following these rules: write exactly 2-3 complete sentences in one paragraph; no bullet points, no numbering, no lists; do not use absolute uniqueness claims like “only”, “no other”, “unique in the scene”; use hedging like “appears to be”, “as far as visible”, “likely”; do not reference frame numbers (use “early/mid/late” if needed); do not mention any visual markers or annotations; keep the factual content but improve the format.

Output ONLY the rewritten caption, no preamble.

Prompt for Temporal Synthesis:**[Video-Level Synthesis]**

You are given {num_batches} temporal descriptions of a video scene, each covering a different time period (separated by —). Synthesize them into a coherent 2-4 sentence description that captures:

- Overall environment and lighting conditions
- Camera characteristics and movement patterns
- Object density and occlusion patterns
- Tracking challenges across the entire video

Temporal descriptions (separated by —):

{batch_descriptions}

CRITICAL REQUIREMENTS:

- Write exactly 2-4 complete sentences in ONE paragraph
- NO bullet points, NO numbering, NO lists
- Preserve important details from all temporal segments
- Focus on consistent patterns and overall characteristics
- Do NOT reference batch numbers, segment numbers, or time periods explicitly
- Output ONLY the synthesized description in English; no preamble

[Instance-Level Synthesis]

You are given {num_batches} temporal descriptions of a tracked object, each covering a different time period (separated by —). Synthesize them into a coherent 2-3 sentence description that captures:

- Distinctive visual features (appearance, clothing, accessories)
- Size and shape characteristics
- MOVEMENT PATTERN (trajectory, speed, stopping/starting) - this is KEY to distinguishing similar objects
- Position changes and spatial relationships
- Interactions with other objects
- Temporal changes in appearance or behavior

Temporal descriptions (separated by —):

{batch_descriptions}

CRITICAL REQUIREMENTS:

- Write exactly 2-3 complete sentences in ONE paragraph
- NO bullet points, NO numbering, NO lists
- Provide 2-3 unique identifiers; avoid absolute uniqueness claims
- Use hedging: “appears to be”, “as far as visible”, “likely”
- Preserve discriminative details from all temporal segments
- Do NOT reference batch numbers, segment numbers, or time periods explicitly
- Output ONLY the synthesized description in English; no preamble

H.3 Prompts for Datasets Evaluation

To rigorously validate our model selection while managing computational overhead, we utilize GPT-4o as an impartial automated judge. To ensure statistical significance, we sampled a representative subset for evaluation: 300 sequences from the BenSMOT dataset (approximately 10% of the training set) and 100 sequences from the TAO dataset, accounting for the extreme sequence lengths in the latter.

Unlike generic captioning metrics, our evaluation focus shifts towards four key dimensions: **Completeness** (coverage of entities and scenes), **Internal Consistency** (logical flow), **Clarity** (readability), and **Faithfulness** (adherence to ground truth or reference context). Below, we provide the specific system prompts used for the two primary datasets.

Prompt for TAO Evaluation (Versatile Mode):

You are a strict and objective text-quality judge for dataset caption evaluation.

Task type: {task_type} | **Evaluation mode:** {evaluation_mode}

[Rules]

1. Only judge based on the provided text input. Do not browse the web or read external files.
2. Return ONLY valid JSON following the schema. No markdown, no prose.
3. All scores must be in [0, 10]. Decimal values are allowed.

4. **Completeness:** Coverage of important entities, scene context, and verifiable details.
5. **Internal Consistency:** Self-consistency and logical coherence within each text.
6. **Clarity:** Readability, sentence quality, and unambiguous references.
7. **Faithfulness (Pair-mode only):** Treat the counterpart as ground truth; penalize invented or contradictory concrete details. Omission alone is not a faithfulness error (penalize completeness instead).

[Input Data]
 {input_block}

Prompt for BenSMOT Evaluation (Comparative Pair Mode):

You are a strict and objective text-quality judge for dataset caption evaluation.

Task type: {task_type}

[Scoring Rubric]

- **9.0 - 10.0:** Flawless / Excellent.
- **7.0 - 8.9:** Good, but with minor issues or slight redundancy.
- **5.0 - 6.9:** Mediocre, containing noticeable errors or significant omissions.
- **< 5.0:** Poor, severe hallucinations, or completely illogical.

[Evaluation Logic]

1. **Notes First:** Generate the “notes” field FIRST to reason through the evaluation before assigning numeric scores.
2. **Faithfulness (Strictly Directional):**
 - *faithfulness_A_to_B*: Assume B is absolute ground truth. Does A invent things not in B?
 - *faithfulness_B_to_A*: Assume A is absolute ground truth. Does B invent things not in A?
3. **Constraint:** Do not reward guessed details. If details conflict with the counterpart, aggressively lower faithfulness and do not inflate completeness.

[Input Data]

Text A: {text_A}

Text B: {text_B}

H.4 Prompts for Fine-grained GPT-4o Evaluation

Fine-grained GPT-4o Evaluation Prompts (Video-ChatGPT’s way):

To evaluate the five fine-grained semantic dimensions (Correctness, Detail Orientation, Contextual Understanding, Temporal Understanding, and Consistency), we adapt the established Video-ChatGPT evaluation prompts. The prompts consist of a System Prompt defining the judge’s role and rules, and a User Prompt providing the input data.

1. Correctness of Information

[System Prompt]

You are an intelligent chatbot designed for evaluating the factual accuracy of generative outputs for video-based description pairs. Your task is to compare the predicted description with the correct description and determine if they are factually consistent. Here is how you can accomplish the task:

INSTRUCTIONS:

- Focus on the factual consistency between the predicted description and the correct description. The predicted description should not contain any misinterpretations or misinformation.
- The predicted description must be factually accurate and align with the video content.
- Consider synonyms or paraphrases as valid matches.
- Evaluate the factual accuracy of the prediction compared to the correct description.

[User Prompt]

Please evaluate the following video-based description pair:

Question: {question}

Correct Description: {answer}

Predicted Description: {pred}

Provide your evaluation only as a factual accuracy score where the factual accuracy score is an integer value between 0 and 5, with 5 indicating the highest level of factual consistency. Please generate the response in the form of a Python dictionary string with keys 'score', where its value is the factual accuracy score in INTEGER, not STRING. DO NOT PROVIDE ANY OTHER OUTPUT TEXT OR EXPLANATION. Only provide the Python dictionary string. For example, your response should look like this: {'score': 4}.

2. Detail Orientation

[System Prompt]

You are an intelligent chatbot designed for evaluating the detail orientation of generative outputs for video-based description pairs. Your task is to compare the predicted description with the correct description and determine its level of detail, considering both completeness and specificity. Here is how you can accomplish the task:

INSTRUCTIONS:

- Check if the predicted description covers all major points from the video. The response should not leave out any key aspects.
- Evaluate whether the predicted description includes specific details rather than just generic points. It should provide comprehensive information tied to specific elements of the video.
- Consider synonyms or paraphrases as valid matches.
- Provide a single evaluation score that reflects the level of detail orientation, considering both completeness and specificity.

- Do NOT give higher scores simply because the predicted description is longer. Only reward details that are consistent with the correct description.

[User Prompt]

(Input format identical to Correctness, requesting an integer detail orientation score between 0 and 5.)

3. Contextual Understanding

[System Prompt]

You are an intelligent chatbot designed for evaluating the contextual understanding of generative outputs for video-based description pairs. Your task is to compare the predicted description with the correct description and determine if the generated response aligns with the overall context of the video content. Here is how you can accomplish the task:

INSTRUCTIONS:

- Evaluate whether the predicted description aligns with the overall context of the video content. It should not provide information that is out of context or misaligned.
- The predicted description must capture the main themes and sentiments of the video.
- Consider synonyms or paraphrases as valid matches.
- Provide your evaluation of the contextual understanding of the prediction compared to the correct description.

[User Prompt]

(Input format identical to Correctness, requesting an integer contextual understanding score between 0 and 5.)

4. Temporal Understanding

[System Prompt]

You are an intelligent chatbot designed for evaluating the temporal understanding of generative outputs for video-based description pairs. Your task is to compare the predicted description with the correct description and determine if they correctly reflect the temporal sequence of events in the video content. Here is how you can accomplish the task:

INSTRUCTIONS:

- Focus on the temporal consistency between the predicted description and the correct description. The predicted description should correctly reflect the sequence of events as they are presented in the video content.
- Consider synonyms or paraphrases as valid matches, but only if the temporal order is maintained.
- Evaluate the temporal accuracy of the prediction compared to the correct description.

[User Prompt]

(Input format identical to Correctness, requesting an integer temporal accuracy score between 0 and 5.)

5. Consistency**[System Prompt]**

You are an intelligent chatbot designed for evaluating the consistency of generative outputs for similar video-based description pairs. You will be given two very similar questions, a common correct description and predicted descriptions for the two questions. Your task is to compare the predicted descriptions and determine if they are consistent. Here is how you can accomplish the task:

INSTRUCTIONS:

- Focus on the consistency between the two predicted descriptions and the correct description. Both predicted descriptions should correspond to the correct description and to each other, and should not contain contradictions.
- Both predicted descriptions must be consistent with each other and the correct description, in terms of the information they provide about the video content.
- Consider synonyms or paraphrases as valid matches, but only if they maintain consistency in conveyed information.
- Evaluate the consistency of the two predicted descriptions compared to the correct description.

[User Prompt]

Please evaluate the following video-based description pair:

Question 1: {question1}

Question 2: {question2}

Correct Description: {answer}

Predicted Description to Question 1: {pred1}

Predicted Description to Question 2: {pred2}

Provide your evaluation only as a consistency score where the consistency score is an integer value between 0 and 5, with 5 indicating the highest level of consistency. *(Formatting constraints identically follow the previous dimensions).*